

# Journal of Materials Chemistry A

Accepted Manuscript



This article can be cited before page numbers have been issued, to do this please use: A. Yu. Mitrofanov, S. Brandès, F. Herbst, S. Rigolet, A. Lemeune and I. P. Beletskaya, *J. Mater. Chem. A*, 2017, DOI: 10.1039/C7TA01195D.



This is an Accepted Manuscript, which has been through the Royal Society of Chemistry peer review process and has been accepted for publication.

Accepted Manuscripts are published online shortly after acceptance, before technical editing, formatting and proof reading. Using this free service, authors can make their results available to the community, in citable form, before we publish the edited article. We will replace this Accepted Manuscript with the edited and formatted Advance Article as soon as it is available.

You can find more information about Accepted Manuscripts in the [author guidelines](#).

Please note that technical editing may introduce minor changes to the text and/or graphics, which may alter content. The journal's standard [Terms & Conditions](#) and the ethical guidelines, outlined in our [author and reviewer resource centre](#), still apply. In no event shall the Royal Society of Chemistry be held responsible for any errors or omissions in this Accepted Manuscript or any consequences arising from the use of any information it contains.

## Immobilization of copper complexes with (1,10-phenanthroline)phosphonates on titania supports for sustainable catalysis

Alexander Mitrofanov,<sup>a,b</sup> Stéphane Brandès,<sup>a</sup> Frédéric Herbst,<sup>c</sup> Séverinne Rigolet,<sup>d</sup>  
Alla Bessmertnykh-Lemeune,<sup>a,\*</sup> Irina Beletskaya<sup>b,\*</sup>

<sup>a</sup> Institut de Chimie Moléculaire de l'Université de Bourgogne (ICMUB), UMR CNRS 6302, 9 Av. Alain Savary, 21078 Dijon, France. E-mail: [Alla.Lemeune@u-bourgogne.fr](mailto:Alla.Lemeune@u-bourgogne.fr)

<sup>b</sup> Department of Chemistry, Lomonosov Moscow State University, Leninskie Gory, GSP-1, Moscow 119991, Russia. E-mail: [beletska@org.chem.msu.ru](mailto:beletska@org.chem.msu.ru)

<sup>c</sup> Laboratoire Interdisciplinaire Carnot de Bourgogne, UMR CNRS 6303, 9 Av. Alain Savary, 21078 Dijon, France

<sup>d</sup> Institut de Science des Matériaux de Mulhouse, Université de Haute-Alsace, UMR CNRS 7361, 15 rue Jean Starcky, Mulhouse, 68057, France

Different strategies for the immobilization of copper complexes with 1,10-phenanthroline (**phen**) using the phosphonate anchoring group were investigated to prepare robust and porous heterogeneous catalysts. Homoleptic and heteroleptic copper(I) complexes with **phen** bearing the bis(trimethylsiloxy)phosphoryl anchoring group (**Pphen-Si**) at different positions of **phen** backbone were prepared and covalently incorporated into titania (TiO<sub>2</sub>) xerogels by using the sol-gel process or grafted onto a surface of mesoporous TiO<sub>2</sub> (S<sub>BET</sub> = 650 m<sup>2</sup> g<sup>-1</sup>). Copper(I) bis(**Pphen-Si**) complexes were the only complexes that were successfully anchored onto TiO<sub>2</sub> surface because the heterogenization was often accompanied by undesirable dissociation of copper complexes. Hybrid materials based on copper(I) chelates with one **phen** ligand were obtained following a two-step procedure involving the immobilization of **Pphen-Si** chelators and their successive complexation with copper(I) ions. Most porous material **Cu/6b/SM/A** displaying BET surface area of 243 m<sup>2</sup> g<sup>-1</sup> and bearing 0.57 mmol g<sup>-1</sup> of the complex was synthesized according to the surface modification of TiO<sub>2</sub>. Excellent catalytic performance of the reusable **Cu/6b/SM/A** material in the Sonogashira-type coupling and the Huisgen 1,3-dipolar cycloaddition was also demonstrated. This solid represents the first example of mesoporous TiO<sub>2</sub>-supported transition metal catalysts.

## Introduction

Copper catalysts could replace precious metal complexes in many industrial processes involving in pharmaceutical, dye and polymer productions.<sup>1-3</sup> This is of major importance in view of societal concerns relating to environmental and sustainable chemistry. Last two decades, significant improvements in homogeneous Cu-catalysed C–C<sup>4-7</sup> and C–Het (Het = O, S, Se, N, P)<sup>6,8</sup> cross-coupling reactions, additions to unsaturated C–C bonds,<sup>9</sup> the Huisgen 1,3-dipolar cycloaddition,<sup>10</sup> and other organic transformations<sup>2,9,11-15</sup> were reported. Homogeneous catalysts are well suited for increasing the reaction scope and fine tuning the reaction rate and its selectivity. However, the separation of organic products from toxic copper compounds are particularly troublesome<sup>16,17</sup> due to exceptional coordination properties of this metal, which avidly bind a huge range of organic molecules containing oxygen and nitrogen donor sites. To solve this problem and recover the catalyst, several strategies were explored. It was reported that copper nanoparticles and copper-modified dendrimers can

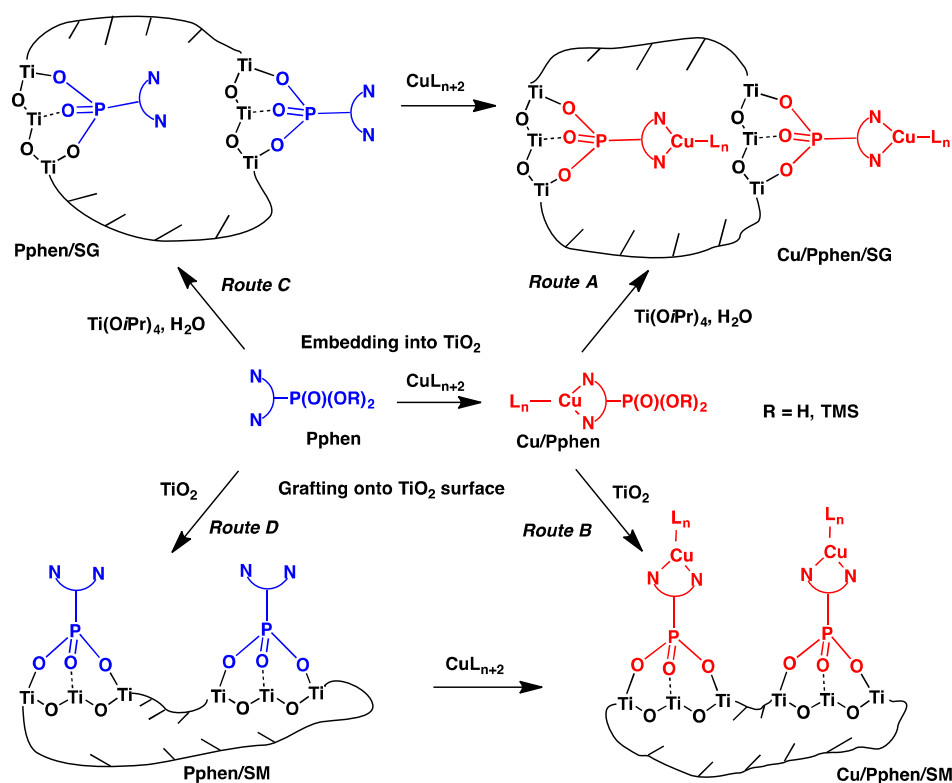
occasionally replace homogeneous catalysts.<sup>18,19</sup> However, their use in industrial processes is also hampered by the difficult purification of products from catalysts. Consequently, copper nanoparticles, salts and oxides were immobilized onto insoluble supports, either organic (polystyrene,<sup>20,21</sup> polyaniline<sup>22</sup> and cellulose<sup>23</sup>) or inorganic (zeolites,<sup>24</sup> hydrotalcite,<sup>25,26</sup> hydroapatites,<sup>27</sup> fluorapatites,<sup>28</sup> silica,<sup>20,29,30</sup> alumina<sup>31-34</sup> and other<sup>35-38</sup>). In these materials, copper ions or nanoparticles are weakly bonded to the solid supports bearing hydroxy, sulfonate or amine coordinating sites. These catalysts benefit from a spatial separation of catalytic species and can be easily recovered, but their stability is quite low. As a result, copper leaching is observed that leads to metal contamination of products and the decrease in the catalytic activity of the recovered solids.

Another promising approach to robust catalytic materials is a direct immobilization of relevant copper complexes onto solid supports such as silicas,<sup>21,39-41</sup> zeolites,<sup>42</sup> metal-organic frameworks (MOFs)<sup>43</sup> or graphene.<sup>44</sup> For instance, heterogenized copper N,N- and N,O-chelates (Cu/L) were applied as catalysts in the Huisgen cycloaddition,<sup>21,41,45</sup> the Mannich three-component coupling reaction,<sup>46</sup> the Sonogashira-type coupling,<sup>47</sup> the Ullmann-type arylation of amines,<sup>48</sup> the oxidative carbonylation of methanol<sup>49</sup> and other organic transformations. Surprisingly, catalyst leaching is difficult to control even for these materials. As a result, it is still a common industrial practice to avoid, whenever possible, the use of copper catalysts, in particular during the later steps of the synthesis of complex molecules in pharmaceutical and agrochemical industries. There is thus a need to develop more efficient immobilization strategies for the heterogenization of copper chelates.

The choice of the solid support is a key point for the efficient catalyst immobilization. Inorganic supports offer various inherent advantages over organic and biopolymers. They are insoluble in common organic solvents and water, do not swell and display a high structural, thermal, mechanical and chemical stability. Rigid structure of these supports allows for a spatial separation of catalytic centres. Recent investigations of hybrid organic-inorganic materials based on phosphonates revealed that metal oxides or polymeric phosphonate networks can be used as a solid support for heterogenization of transition metal complexes.<sup>49-52</sup> Among them, TiO<sub>2</sub> are particularly interesting because resulting molecular materials are cost-effective and display exceptional thermal and chemical stability stemming from the robustness of Ti–O(P) and P–C bonds. Several strategies are currently available for immobilization of phosphonates onto TiO<sub>2</sub> supports including sol-gel (SG) processes and surface modification (SM) reactions.<sup>53-55</sup> Examples of TiO<sub>2</sub>-supported transition metal catalysts are still limited to a few reports. Immobilization of palladium complexes with phosphine ligands bearing phosphonate anchoring groups on TiO<sub>2</sub> matrices was carefully studied but all obtained materials were inefficient in the Sonogashira coupling reaction.<sup>56</sup> Ru(II) and Ir(I) complexes with bipyridine were incorporated into TiO<sub>2</sub> matrices in order to prepare heterogeneous catalysts for reduction of aromatic and unsaturated ketones.<sup>53,57</sup> Under appropriate conditions, these solids catalysed heterogeneous hydrogenation with practically useful chemoselectivity. The titania-supported Co(I) complex prepared by using SG method was an efficient catalyst for the hydroformylation of alkenes in contrast to a relevant homogeneous complex.<sup>58</sup> It has to be noted that all reported hybrid materials based on titania were non-porous since they displayed low specific surface areas (< 100 m<sup>2</sup> g). This is a serious drawback for their catalytic performance.

In the present work, we report the heterogenization of copper complexes with **phen** ligands bearing the phosphonate anchoring group using titania matrices. This approach to the immobilization of copper catalysts combines several potential advantages including thermodynamic stability of copper chelates with **phen** ligands, their catalytic efficiency and versatility, the strong covalent linkage of phosphonates to TiO<sub>2</sub> networks and excellent mechanical, thermal and chemical properties of titania, which is widely used in industry as a

support for inorganic catalysts. In particular, we were interested to control the porosity of the materials and prepare cost-effective solid catalysts with surface characteristics that are relatively close to those of mesoporous materials commonly used as heterogenized catalysts such as functionalized ordered silicas. In this regard, the immobilization of **pphen** ligands functionalized by the phosphonate group (**Pphen**) and their copper(I) complexes (**Cu/Pphen**) was investigated in details. First, **Pphen/SG** and **Cu/Pphen/SG** materials were prepared reacting **Pphen** ligands or their complexes with titanium isopropoxide ( $\text{Ti}(\text{OiPr})_4$ ) according to the SG process (Scheme 1, routes A and C, Figure 1). Alternatively, these ligands and complexes were grafted onto the surface of mesoporous titanium oxide ( $S_{\text{BET}} = 650 \text{ m}^2 \text{ g}^{-1}$ ) yielding **Pphen/SM** and **Cu/Pphen/SM** materials (Scheme 1, routes B and D, Figure 1). Moreover, the complexation of copper ions with **Pphen/SM** solids was explored to prepare heterogenized chelates. The structural characteristics of hybrid materials and the integrity of the immobilized molecules were investigated by different physicochemical methods, including elemental analysis, infrared spectroscopy, nitrogen sorption isotherms, EDX spectrometry, scanning electron microscopy (SEM), transmission electron microscopy (TEM) and solid-state NMR. Finally, the catalytic performance of most porous material **Cu/6b/SM/A** was examined



**Scheme 1.** Schematic representation of the immobilization of copper complexes with **pphen** ligands according to the SG process (routes A and C) and the SM reaction (routes B and D).

in the Sonogashira-type and Huisgen cycloaddition reactions. These studies demonstrated that **Cu/6b/SM/A** is stable in the presence of strong bases like triethylamine and cesium carbonate and efficient as a catalyst for both reactions. This solid catalyst can be readily recovered and reused up to 10 times without loss of activity. To the best of our knowledge, this is the first

example of *mesoporous* titania-supported transition metal catalysts.

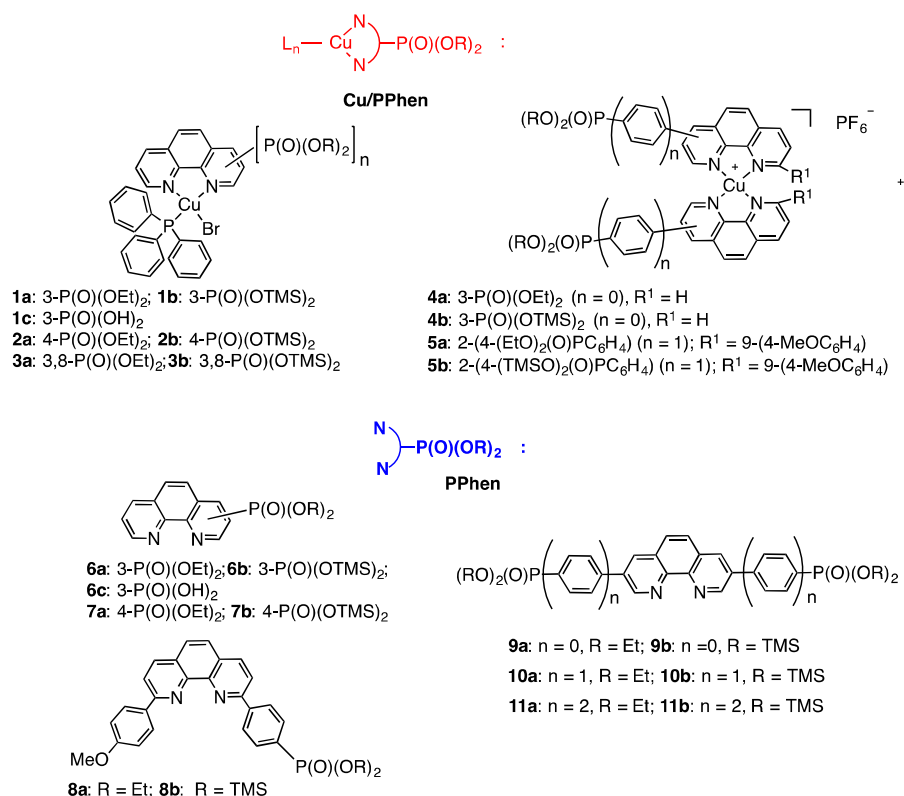


**Figure 1.** Structures of **Pphen** ligands and **Cu/Pphen** complexes.

## Experimental

Unless otherwise noted, all chemicals and starting materials were obtained commercially from Acros® or Aldrich® and used without further purification. Complex Cu(PPh<sub>3</sub>)<sub>3</sub>Br,<sup>59</sup> 3,8-dibromo-1,10-phenanthroline,<sup>60</sup> 2-chloro-9-(4-methoxyphenyl)-1,10-phenanthroline,<sup>61</sup> 4-(diethoxyphosphoryl)phenylboronic acid pinacol ester<sup>62</sup> and 4-(diethoxyphosphorylphenyl)-4'-phenylboronic acid pinacol ester<sup>62</sup> were prepared according to literature methods. Mesoporous TiO<sub>2</sub> was synthesized from Ti(OiPr)<sub>4</sub> according to the sol-gel process in the presence of limited amount of water (20 equiv) in THF (see the Supporting Information).<sup>63</sup> The empirical formula of hydrated TiO<sub>2</sub> ((TiO<sub>x</sub>(OH)<sub>4-2x</sub>)·m(H<sub>2</sub>O)·n(iPrOH), x = 1.6-1.8; m = 0.1-0.4; y = 0.1-0.2) was calculated based on the elemental analysis of xerogel dried at 80 °C under reduced pressure for 12 h.

Phenanthrolyl phosphonates **6a-8a**,<sup>64</sup> heteroleptic copper(I) complexes Cu(Pphen)(PPh<sub>3</sub>)Br (**1a-3a**)<sup>65</sup> and homoleptic complex [Cu(Pphen)<sub>2</sub>]PF<sub>6</sub> (**4a**)<sup>65</sup> were obtained according to our previous reports.

Analytical thin-layer chromatography (TLC) was carried out using Merck silica gel 60 plates (precoated sheets, 0.2 mm thick, with fluorescence indicator F254). Column chromatography purification was carried out on silica gel (Silica 60, 63-200 μm, Aldrich) and neutral alumina (Aluminium oxide 90, 63-200 μm, Merck). Centrifugation was performed at 6000 rpm for 5 min. Catalytic reactions were carried out using Carousel 12 Plus equipment for parallel synthesis (Radleys).



$^1\text{H}$ ,  $^{31}\text{P}$  and  $^{13}\text{C}$  NMR spectra were acquired either on a Bruker Avance III 500 MHz or a Bruker Avance III Nanobay 300 MHz spectrometer. Chemical shifts are expressed in parts per million (ppm) and referenced to residual non-deuterated solvent signals.<sup>66,67</sup> The coupling constants are expressed in unit of frequency (Hz). The unambiguous assignment of signals in  $^1\text{H}$  and  $^{13}\text{C}$  NMR spectra was performed using gradient-enhanced COSY, HMQS and NOESY correlation experiments. MALDI-TOF mass-spectra were obtained on a Bruker Ultraflex II LRF 2000 mass-spectrometer in positive ion mode with dithranol matrix. Accurate mass measurements (HRMS) were made on a THERMO LTQ Orbitrap XL. Microanalyses (CHN) were performed on a Thermo Finnigan Flash 1112 analyser. Cu, P and Ti elemental analyses were performed with inductively coupled plasma optical emission spectrometers ICP-OES (DUO) ICAP 7400. FTIR spectra were registered on FT-IR Nexus (Nicolet) and Bruker Vector 22 spectrophotometers. Micro-ATR accessory (Pike) was used in order to obtain FTIR spectra of polycrystalline solid complexes. Thermogravimetric (TGA) measurements were performed on a Netzsch STA 409 PC Luxx analyser. Samples were purged in an  $\text{N}_2$  (30 mL  $\text{min}^{-1}$ ) /  $\text{O}_2$  (10 mL  $\text{min}^{-1}$ ) stream during analysis and heated to 1000 °C in alumina crucibles with a heating rate of 10 K  $\text{min}^{-1}$ . Powder X-ray diffraction experiments were performed on an Empyrean diffractometer from the PANalytical company in the range  $3^\circ < 2\theta < 50^\circ$ . The uncrushed samples (few milligrams) were placed between two Mylar sheets and the analysis was performed in transmission mode using a focusing X-ray mirror equipped with fixed divergent and anti-scattering slits (aperture  $0.5^\circ$ ) and 0.02 rad Soller slits. The data collection was run with a copper anticathode X-ray tube ( $\text{Cu } K\alpha_1 = 1.54060 \text{ \AA}$  /  $\text{Cu } K\alpha_2 = 1.54443 \text{ \AA}$ ) and with a X'Celerator detector equipped with an anti-scattering slit of 5 mm. Accurate mass measurements (HRMS) were recorded on a Thermo LTQ Orbitrap XL apparatus equipped with an electrospray ionisation (ESI) source. Nitrogen adsorption-desorption isotherms were measured with Micromeritics ASAP 2010 or 2020 analyser at 77 K with samples outgassed at 393 K in reduced pressure ( $10^{-5}$  torr) for at least 6 h. Specific surface areas were calculated by the BET method.<sup>68</sup> Mesopore characterizations were performed by the Barrett-Joyner-Halenda method.<sup>69</sup> Diffuse reflectance spectra were recorded in the solid state at room temperature on a Agilent Carry 5000 UV-Vis-NIR spectrometer. Continuous wave (CW) EPR spectra of solid samples were recorded on a Bruker ELEXSYS 500. The instrument was equipped with a 4122 SHQE/0405 X-band resonant cavity operating at 9.43 GHz, a X-band high power dual gun-oscillator bridge, and a quartz cryostat cooled at 100 K with a stream of nitrogen. The temperature was regulated with an ER 4131VT accessory. All apparatus as well as the data acquisition were controlled using Xepr software. The magnetic field was swept from 250 to 360 mT through 2048 points. Spectra were recorded at 6 mW power, 100 kHz frequency modulation, 0.5 mT modulation amplitude, 10 ms time constant and 40 ms conversion time. The  $^{31}\text{P}$  solid-state NMR experiment was performed at room temperature on Bruker Avance II 400 spectrometer operating at  $B_0 = 9.4\text{T}$  equipped with a Bruker double channel 4mm probe at a Larmor frequency of 161.99MHz. The spectrum was recorded with a  $\pi/2$  pulse duration of 3.5  $\mu\text{s}$  and a recycling delay of 60 s at a spinning frequency of 14 kHz.  $^{31}\text{P}$  spin lattice relaxation times ( $T_1$ ) was measured with the saturation-recovery pulse sequence.  $^{31}\text{P}$  spectrum was referenced to  $\text{H}_3\text{PO}_4$  (85% in water). Deconvolutions of the spectrum was performed using Dmfit software (<http://nmr.cemhti.cnrs-orleans.fr/dmfit/>) with Gaussian/Lorentzian functions. Field-emission scanning electron microscopy (FESEM) was realized using a JEOL JSM 7600F instrument located in the ARCEN analysis centre of the University of Bourgogne (Dijon). Images were made using GentleBeam-High SEM mode. Transmission electron microscopy (TEM) analyses were conducted using a JEOL JEM-2100F microscope operating at 200 kV and located in the ARCEN analysis centre of the University of Bourgogne (Dijon). EDX spectrometry in STEM and TEM mode was used for chemical

mapping and qualitative elemental analysis using a Bruker XFlash Detector 5030 spectrometer fitted on the JEM-2100F microscope.

All measurements except SEM and TEM imaging and solid state NMR were performed at the "Pôle Chimie Moléculaire", the technological platform for chemical analysis and molecular synthesis (<http://www.wpcm.fr>) which relies on the Institute of the Molecular Chemistry of University of Burgundy and Welience<sup>TM</sup>, a Burgundy University private subsidiary.

### Synthesis of 1,10-phenanthroline phosphonates and complex 5a.

**Diethyl (4-(9-(4-methoxyphenyl)-1,10-phenanthroline-2-yl)phenyl)phosphonate (8a).** A mixture of 2-chloro-9-(4-methoxyphenyl)-1,10-phenanthroline (160 mg, 0.5 mmol), 4-(diethoxyphosphoryl)phenylboronic acid pinacol ester (187 mg, 0.55 mmol), Pd(dppf)Cl<sub>2</sub> (20.4 mg, 0.025 mmol) and Cs<sub>2</sub>CO<sub>3</sub> (815 mg, 2.5 mmol) in dioxane was stirred for 3 h at reflux under Ar. The mixture was filtered and concentrated under reduced pressure. The residue was purified by column chromatography on silica gel (eluent CH<sub>2</sub>Cl<sub>2</sub>/MeOH (0–1% MeOH in CH<sub>2</sub>Cl<sub>2</sub>)). Beige solid. Yield 70% (174 mg).  $\nu_{\max}/\text{cm}^{-1}$  2982 (CH), 2937 (CH), 2905 (CH), 1602, 1587, 1578, 1544, 1488, 1441, 1421, 1392, 1362, 1300, 1246 (P = O), 1174, 1133, 1113, 1095, 1016 (POC), 958 (POC), 891, 837, 792, 780, 746.  $\delta_{\text{H}}$  (300 MHz, CDCl<sub>3</sub>, 300 K) 1.38 (t,  $^3J_{\text{H,H}}$  7.1, 6H, Me), 3.95 (s, 3H, OMe), 4.19 (m, 4H, CH<sub>2</sub>), 7.14 (d,  $^3J_{\text{H,H}}$  8.8, 2H, *m*-H), 7.79 (AB-system,  $J_{\text{AB}}$  8.7, 2H, 5,6-H), 8.06 (dd,  $^3J_{\text{H,P}}$  13.0,  $^3J_{\text{H,H}}$  8.3, 2H, *m*-H), 8.13 (d,  $^3J_{\text{H,H}}$  8.7, 1H, 8-H), 8.18 (d,  $^3J_{\text{H,H}}$  8.7, 1H, 3-H), 8.30 (d,  $^3J_{\text{H,H}}$  8.7, 1H, 7-H), 8.37 (d,  $^3J_{\text{H,H}}$  8.7, 1H, 4-H), 8.45 (d,  $^3J_{\text{H,H}}$  8.8, 2H, *o*-H), 8.57 (dd,  $^3J_{\text{H,H}}$  8.3,  $^4J_{\text{H,P}}$  3.9, 2H, *o*-H).  $\delta_{\text{C}}$  (125 MHz, CDCl<sub>3</sub>, 300 K) 16.4 (d,  $^3J_{\text{C,P}}$  6, 2C, Me), 55.4 (1C, OMe), 62.2 (d,  $^2J_{\text{C,P}}$  5, 2C, OCH<sub>2</sub>), 114.3 (2C, *m*-C), 119.6 (1C, 8-C), 120.0 (1C, 3-C), 125.4 (1C, 6-C), 126.7 (1C, 5-C), 127.5 (1C, 4a or 6a-C), 127.7 (d,  $^3J_{\text{C,P}}$  15, 2C, *o*-C), 128.3 (1C, 4a or 6a-C), 128.8 (d,  $^1J_{\text{C,P}}$  187, 1C, *ipso*-C), 129.0 (2C, *o*-C), 132.0 (1C, *p*-C), 132.4 (d,  $^2J_{\text{C,P}}$  10, 2C, *m*-C), 136.8 (1C, 7-C), 137.1 (1C, 4-C), 143.4 (d,  $^4J_{\text{C,P}}$  3, 1C, *p*-C), 146.0 (1C, 10a or 10b-C), 146.1 (1C, 10a or 10b-C), 155.3 (1C, 2 or 9-C), 156.4 (1C, 2 or 9-C), 161.0 (1C, *p*-C).  $\delta_{\text{P}}$  (121 MHz, CDCl<sub>3</sub>, 300 K) 18.82. HRMS (ESI): *m/z*: found: 521.1586; calc. for C<sub>29</sub>H<sub>27</sub>N<sub>2</sub>NaO<sub>4</sub>P ([M+Na]<sup>+</sup>): 521.1601.

**Tetraethyl ((1,10-phenanthroline-3,8-diyl)bis(4,1-phenylene))bis(phosphonate) (10a).** A mixture of 3,8-dibromo-1,10-phenanthroline (169 mg, 0.5 mmol), 4-(diethoxyphosphoryl)phenylboronic acid pinacol ester (425 mg, 1.25 mmol), Pd(OAc)<sub>2</sub> (11.2 mg, 0.05 mmol), PPh<sub>3</sub> (40 mg, 0.15 mmol) and Cs<sub>2</sub>CO<sub>3</sub> (815 mg, 2.5 mmol) in dioxane (4 ml) was stirred at reflux for 40 h under Ar. The reaction mixture was cooled to room temperature and filtered. The filtrate was concentrated under reduced pressure and the residue was purified by column chromatography on silica gel (eluent – CH<sub>2</sub>Cl<sub>2</sub>). White solid. Yield 52% (155 mg).  $\nu_{\max}/\text{cm}^{-1}$  2983 (CH), 1603, 1556, 1475, 1432, 1392, 1365, 1244 (P = O), 1163, 1132, 1099, 1042, 1014 (POC), 959 (POC), 937, 838, 815, 793, 762, 731.  $\delta_{\text{H}}$  (300 MHz, CDCl<sub>3</sub>, 300 K) 1.34 (t,  $^3J_{\text{H,H}}$  7.1, 12H, Me), 4.15 (m, 8H, CH<sub>2</sub>), 7.86 (dd,  $^3J_{\text{H,H}}$  8.3,  $^4J_{\text{H,P}}$  3.8, 2H, *o*-H), 7.90 (s, 2H, 5,6-H), 7.98 (dd,  $^3J_{\text{H,P}}$  13.0,  $^3J_{\text{H,H}}$  8.3, 2H, *m*-H), 8.42 (d,  $^4J_{\text{H,H}}$  2.3, 2H, 4,7-H), 9.42 (d,  $^4J_{\text{H,H}}$  2.3, 2H, 2,9-H).  $\delta_{\text{C}}$  (125 MHz, CDCl<sub>3</sub>, 300 K) 16.4 (d,  $^3J_{\text{C,P}}$  6 Hz, 4C, Me), 62.3 (d,  $^2J_{\text{C,P}}$  5, 4C, OCH<sub>2</sub>), 127.35 (2C, 5,6-C), 127.6 (d,  $^3J_{\text{C,P}}$  13, 4C, *o*-C), 129.2 (d,  $^1J_{\text{C,P}}$  187, 2C, *ipso*-C), 129.3 (2C, 4a,6a-C), 132.7 (d,  $^2J_{\text{C,P}}$  10, 4C, *m*-C), 133.9 (2C, 4,7-C), 134.9 (2C, 3,8-C), 141.4 (d,  $^4J_{\text{C,P}}$  3, 2C, *p*-C), 145.5 (2C, 10a,10b-C), 149.4 (2C, 2,9-C).  $\delta_{\text{P}}$  (121 MHz, CDCl<sub>3</sub>, 300 K) 18.14. HRMS (ESI): *m/z* found: 605.1944; calc. for C<sub>32</sub>H<sub>34</sub>N<sub>2</sub>NaO<sub>6</sub>P<sub>2</sub> ([M+H]<sup>+</sup>): 605.1965.

**Tetraethyl ((1,10-phenanthroline-3,8-diyl)bis([1,1'-biphenyl]-4',4-diyl))bis(phosphonate) (11a).** A mixture of 3,8-dibromo-1,10-phenanthroline (169 mg, 0.5 mmol), 4-((diethoxyphosphoryl)phenyl)-4'-phenylboronic acid pinacol ester (520 mg, 1.25 mmol),

$\text{Pd}(\text{OAc})_2$  (11.2 mg, 0.05 mmol),  $\text{PPh}_3$  (40 mg, 0.15 mmol) and  $\text{Cs}_2\text{CO}_3$  (815 mg, 2.5 mmol) in dioxane (4 mL) was stirred at reflux for 24 h under Ar. The reaction mixture was cooled and filtered. The filtrate was concentrated under reduced pressure. The residue was purified by column chromatography on silica gel (eluent –  $\text{CH}_2\text{Cl}_2$ ). White solid. Yield 76% (226 mg).  $\nu_{\text{max}}/\text{cm}^{-1}$  2985 (CH), 1601, 1493, 1476, 1434, 1388, 1367, 1236 (P = O), 1162, 1132, 1050, 1017 (POC), 939, 917, 848, 822, 780, 733, 695.  $\delta_{\text{H}}$  (300 MHz,  $\text{CDCl}_3$ , 300 K) 1.34 (t,  $^3J_{\text{H,H}}$  7.1, 12H, Me), 4.15 (m, 8H,  $\text{CH}_2$ ), 7.72–7.94 (m, 18H), 8.42 (d,  $^4J_{\text{H,H}}$  2.3, 2H, 4,7-H), 9.46 (d,  $^4J_{\text{H,H}}$  2.3, 2H, 2,9-H).  $\delta_{\text{C}}$  (125 MHz,  $\text{CDCl}_3$ , 300 K) 16.4 (d,  $^3J_{\text{C,P}}$  6, 4C, Me), 62.2 (d,  $^2J_{\text{C,P}}$  5.3, 4C,  $\text{OCH}_2$ ), 126.9 (2C, 5,6-C), 127.19 (d,  $^3J_{\text{C,P}}$  9, 4C, *o*-C), 127.75 (d,  $^1J_{\text{C,P}}$  187, 2C, *ipso*-C), 128.1 (d,  $^3J_{\text{C,P}}$  9, 8C, *m,o*-C), 129.33 (2C, 4a,6a-C), 132.5 (d,  $^2J_{\text{C,P}}$  9, 4C, *m*-C), 133.3 (2C, 4,7-C), 135.1 (2C, 3,8-C), 137.3 (2C, Ar-C), 140.0 (2C, Ar -C), 144.2 (d,  $^4J_{\text{C,P}}$  3, 2C, *p*-C), 145.3 (2C, 10a,10b-C), 149.4 (2C, 2,9-C).  $\delta_{\text{P}}$  (121 MHz,  $\text{CDCl}_3$ , 300 K) 18.70. HRMS (ESI)  $m/z$ : found: 779.2388; calc. for  $\text{C}_{44}\text{H}_{42}\text{N}_2\text{NaO}_6\text{P}_2$  ( $[\text{M}+\text{H}]^+$ ): 779.2410.

**[Cu(8a)<sub>2</sub>]PF<sub>6</sub> (5a).** Phenanthroline phosphonate **8a** (125 mg, 0.25 mmol) was dissolved in dichloromethane ( $\text{CH}_2\text{Cl}_2$ ) (5 mL) under Ar. A solution of  $[\text{Cu}(\text{CH}_3\text{CN})_4]\text{PF}_6$  (46.6 mg, 0.125 mmol) in  $\text{CH}_2\text{Cl}_2$  (10 mL) was prepared under Ar and then added with a syringe to the stirred solution of the ligand. Then the reaction mixture was stirred at room temperature for 10 min, cooled to room temperature and concentrated under reduced pressure. The solid residue was dissolved in  $\text{CH}_2\text{Cl}_2$  (2 mL) and the solution was layered with diethyl ether (10 mL). A precipitate was collected by filtration and then dried under vacuum. Brown crystals. Yield 80% (110 mg).  $\nu_{\text{max}}/\text{cm}^{-1}$  2982 (CH), 2906 (CH), 1605, 1552, 1545, 1490, 1422, 1391, 1358, 1322, 1303, 1247 (P = O), 1175, 1134, 1110, 1042, 1014 (POC), 959 (POC), 904, 867, 834, 782, 750, 722.  $\delta_{\text{H}}$  (500 MHz,  $\text{CD}_2\text{Cl}_2$ , 300 K) 1.26 (t,  $^3J_{\text{H,H}}$  7.1, 12H, Me), 3.45 (s, 6H, OMe), 3.95 (m, 8H,  $\text{CH}_2$ ), 5.99 (d,  $^3J_{\text{H,H}}$  8.4, 4H, *m*-H), 7.04 (dd,  $^3J_{\text{H,P}}$  12.6,  $^3J_{\text{H,H}}$  8.0, 4H, *m*-H), 7.31 (d,  $^3J_{\text{H,H}}$  8.4, 4H, *o*-H), 7.62 (dd,  $^3J_{\text{H,H}}$  8.0,  $^4J_{\text{H,P}}$  2.4, 4H, *o*-H), 7.85 (d,  $^3J_{\text{H,H}}$  8.3, 2H), 7.93 (d,  $^3J_{\text{H,H}}$  8.3, 2H), 8.06 (s, 4H), 8.48 (d,  $^3J_{\text{H,H}}$  8.3, 2H), 8.59 (d,  $^3J_{\text{H,H}}$  8.3, 2H).  $\delta_{\text{P}}$  (121 MHz,  $\text{CD}_2\text{Cl}_2$ , 300 K) 18.81. HRMS (ESI):  $m/z$  found 1059.2703; calc. for  $\text{C}_{58}\text{H}_{54}\text{CuN}_4\text{O}_8\text{P}_2$ : ( $[\text{M}-\text{PF}_6]^+$ ) 1059.2707.

**General procedure for the preparation of silyl phosphonate esters 6b-11b.** To a 0.1 M solution of diethyl phosphonate esters **6a-11a** in dry dichloromethane TMSBr (6 equiv. for each diethoxyphosphoryl group) was added under Ar and the resulting mixture was stirred at room temperature until a complete conversion of diethyl esters according  $^1\text{H}$  NMR spectroscopy (24–48 h). Evaporation of volatiles under reduced pressure afforded silyl phosphonate esters **6b-11b** in quantitative yield. The compounds were introduced in the next step without additional purification.

**Bis(trimethylsilyl) 1,10-phenanthroline-3-ylphosphonate (6b).**  $\delta_{\text{H}}$  (300 MHz,  $\text{CDCl}_3$ , 300 K) 0.25 (s, 18H, Me), 7.65 (dd,  $^3J_{\text{H,H}}$  8.1,  $^3J_{\text{H,H}}$  4.3, 1H, 8-H), 7.82 (d,  $^3J_{\text{H,H}}$  9.2 Hz, 1H, 6-H), 7.85 (d,  $^3J_{\text{H,H}}$  9.2, 1H, 5-H), 8.26 (dd,  $^3J_{\text{H,H}}$  8.1,  $^4J_{\text{H,H}}$  1.7, 1H, 7-H), 8.68 (dd,  $^3J_{\text{H,P}}$  15.2,  $^4J_{\text{H,H}}$  2.0, 1H, 4-H), 9.17 (dd,  $^3J_{\text{H,H}}$  4.3,  $^4J_{\text{H,H}}$  1.7, 1H, 9-H), 9.33 (dd,  $^3J_{\text{H,P}}$  5.4,  $^4J_{\text{H,H}}$  2.0, 1H, 9-H).  $\delta_{\text{P}}$  (121 MHz,  $\text{CDCl}_3$ , 300 K) -3.61.

**(1,10-Phenanthroline-3-yl)phosphonic acid (6c).** To a solution of **6a** (79.1 mg, 0.25 mmol) in dry  $\text{CH}_2\text{Cl}_2$  (2.5 mL) TMSBr (198  $\mu\text{L}$ , 1.5 mmol) was added under Ar and the resulting mixture was stirred at room temperature until a complete conversion of the diethyl ester according  $^1\text{H}$  NMR spectroscopy (24 h). Then MeOH (100  $\mu\text{L}$ ) was added and the reaction mixture was filtered. The precipitate was washed with MeOH (1 mL x 2),  $\text{CH}_2\text{Cl}_2$  (1 mL) and dried under reduced pressure. White solid. Yield 98% (63.7 mg). Found C 55.27, H 3.35, N 10.98. Calc. for  $\text{C}_{12}\text{H}_9\text{N}_2\text{O}_3\text{P}$ : C 55.39; H 3.49; N 10.77 %.  $\delta_{\text{H}}$  (300 MHz,  $\text{CD}_3\text{OD}$ , 300 K) 8.35–8.45 (m, 3H, 5,6,8-H), 9.09 (d,  $^3J_{\text{HP}}$  14.5, 1H, 4-H), 9.31–9.37 (br. m, 2H, 7,9-H), 9.50 (d,  $^3J_{\text{HP}}$  5.5, 1H, 2-H).  $\delta_{\text{P}}$  (300 MHz,  $\text{CD}_3\text{OD}$ , 300 K) 12.16.

**Immobilization of copper complexes Cu/Pphen.**



*General procedure for the preparation of Cu/Pphen/SG xerogels.* Silyl phosphonate ester **6b** or **9b** was dissolved in THF and treated with solid  $\text{Cu}(\text{PPh}_3)_3\text{Br}$  at room temperature for 30 min to obtain complexes **1b** or **3b**, respectively. Then a 0.8 M solution of  $\text{Ti}(\text{OiPr})_4$  in THF was added to yield a transparent coloured solution. After stirring of the resulting mixture for 40 min, water diluted by THF (5 M solution) was added dropwise to this solution. A rapid formation of gels or precipitates was observed. The reaction mixture was kept without stirring for 48 h at room temperature. The precipitate was collected by filtration, washed with THF, methanol and diethyl ether and dried under reduced pressure (2 mmHg) at 80 °C for 24 h. The amount of reagents and solvents employed for the preparation of complexes **1b** and **3b** and in the sol-gel process, yields of **Cu/Pphen/SG** xerogels are summarized in Table S1. Elemental analyses of xerogels **Cu/Pphen/SG** are reported in Tables S2 and S3.

Complex  $\text{Cu}(\text{6b})(\text{PPh}_3)\text{Br}$  (**1b**) is sensitive to moisture and was characterized by  $^1\text{H}$  and  $^{31}\text{P}$  spectroscopy in a crude mixture obtained after evaporation of volatiles. This mixture contains the complex **1b** and  $\text{PPh}_3$ .

**Cu(6b)(PPh<sub>3</sub>)Br (1b).**  $\delta_{\text{H}}$  (300 MHz,  $\text{CDCl}_3$ , 300 K) 0.21 (s, 18H, Me), 7.19 (m, 9H, *m,p*-H), 7.29 (m, 6H, *o*-H), 7.82 (br s, 1H, 8-H), 8.05 (br. d,  $^3J_{\text{H,H}}$  8.8, 1H, 6-H), 8.18 (br. d,  $^3J_{\text{H,H}}$  8.8, 1H, 5-H), 8.65 (br s, 1H, 7-H), 8.75 (br s, 1H, 4-H), 8.80 (br s, 1H, 9-H), 9.15 (br s, 1H, 2-H).  $\delta_{\text{P}}$  (121 MHz,  $\text{CDCl}_3$ , 300 K) -4.67 (br s).

*General procedure for the surface modification of mesoporous titanium oxide.* Silyl phosphonate esters **6b–8b** were dissolved in  $\text{CH}_2\text{Cl}_2$  and treated with solid  $\text{Cu}(\text{PPh}_3)_3\text{Br}$  or  $[\text{Cu}(\text{CH}_3\text{CN})_4]\text{PF}_6$  at room temperature for 30 min under Ar to prepare complexes **1b**, **2b**, **4b** or **5b**. After the reaction was completed, a transparent coloured solution was cannulated into a flask containing  $\text{TiO}_2$  under Ar. The suspension was stirred for 2 days at room temperature. The solid was collected by filtration, washed with THF, methanol and ether and dried for 24 h at 80 °C under reduced pressure (2 mmHg). The amount of reagents and solvents used for the preparation of complexes and the sol-gel process are reported in Table S4. Elemental analyses of solids **Cu/Pphen/SM** are summarized in Tables S5 and S6.

#### Immobilization of ligands PPhen-Si.

*General procedure for the preparation of Pphen/SG xerogels.* Silyl phosphonate ester **6b** or **9b–11b** was dissolved in THF. A 0.8 M solution of  $\text{Ti}(\text{OiPr})_4$  in THF was added to this solution and the reaction mixture was stirred for 40 min. Then water diluted by THF (5 M solution) was added dropwise to this solution. A rapid formation of gels or precipitates was observed. Then the reaction mixture was kept without stirring for 48 h at room temperature. The precipitate was collected by filtration, washed with THF, methanol and diethyl ether and dried under reduced pressure (2 mmHg) at 80 °C for 24 h. The amount of reagents and solvents used for the sol-gel process and yields of xerogels **Pphen/SG** are reported in Table S7. Elemental analyses of solids **Pphen/SG** are presented in Table S8.

*Surface modification of mesoporous  $\text{TiO}_2$  by chelate 6b.* Silyl phosphonate diester **6b** prepared from phosphonate **6a** (316 mg, 1 mmol) was dissolved in  $\text{CH}_2\text{Cl}_2$  (20 mL) under Ar. A transparent uncoloured solution was cannulated into a flask containing hydrated titanium oxide (10 mmol) under Ar. The suspension was stirred for 48 h at room temperature. The solid (959 mg) was collected by filtration, washed with THF, MeOH and ether and dried for 24 h at 80 °C under reduced pressure (2 mmHg). The elemental analysis of solid **6b/SM** is reported in Tables S7 and S8.

#### Complex formation with grafted ligand 6b.

A solution of  $\text{Cu}(\text{PPh}_3)_3\text{Br}$  or  $[\text{Cu}(\text{CH}_3\text{CN})_4]\text{PF}_6$  in  $\text{CH}_2\text{Cl}_2$  was added to material **6b/SM** placed into a Schlenk tube under Ar. The suspension was stirred for 24 h at room temperature. The brown solids were collected by centrifugation, washed with  $\text{CH}_2\text{Cl}_2$ , MeOH and diethyl ether and dried under reduced pressure (2 mmHg) for 24 h at 80 °C.

The amount of reagents and yields of materials **Cu/6b/SM** are reported in Table S9. Elemental analyses of **Cu/6b/SM** are summarized in Tables S10 and S11.

### Catalytic reactions.

*General procedure for Sonogashira-type coupling.* A 8 ml glass vial was charged with alkyne (0.75 mmol), aryl iodide (0.5 mmol), Cs<sub>2</sub>CO<sub>3</sub> (325.8 mg, 1 mmol), **Cu/6b/SM/A** (43 mg, 5 mol% calculated onto the grafted complex), PPh<sub>3</sub> (13.1 mg, 10 mol%) and toluene (2 mL) under Ar. A vial was closed with Teflon cap and the reaction mixture was stirred at reflux for 16 h. After cooling to room temperature, the organic phase was separated by centrifugation, and the solid catalyst was washed with toluene (2 mL) and MeOH (5 mL x 2). The combined toluene phases were evaporated to dryness under reduced pressure. The crude products were analysed by <sup>1</sup>H NMR spectroscopy. Mesitylene was used as an internal standard. The spectral data of coupling products were in good agreement with the literature data.<sup>70-75</sup> The results are summarized in Table 5 (entries 1, 7-16) and Scheme 6.

Recycling of **Cu/6b/SM/A** in the reaction of phenylacetylene with *p*-iodoanisole was carried out. After washing with toluene and MeOH, the catalyst was dried under reduced pressure for 3 h and used in the next reaction cycle as reported above for the freshly prepared **Cu/6b/SM/A**. The results are summarized in Table 5 (entries 3-6).

A hot filtration test was performed for the reaction of phenylacetylene with *p*-iodoanisole (Table 5, entry 2). After 1 h of heating, a half of the reaction mixture was taken by syringe equipped with a Acrodisc® syringe filter with Supor® membrane (pore size 10 μm) and transferred into a 8 ml glass vial under Ar. The vial was charged with Cs<sub>2</sub>CO<sub>3</sub> (163 mg, 0.5 mmol), PPh<sub>3</sub> (6.6 mg, 10 mol%). Then both reaction mixtures were stirred at reflux for additional 12 h and monitored by <sup>1</sup>H NMR spectroscopy. The results are shown in Figure S36.

Reaction of phenylacetylene with *p*-iodoanisole (Table 5, entry 2) was also performed using materials **3b/SG/20** and **3b/SG/10** as catalysts. The material loading was calculated using copper content to obtain 5 mol% of grafted complex. In both cases, complete conversion of aryl halide was not achieved even after 72 h of reflux.

To compare the catalytic activity of materials **1b/SM** and **2b/SM**, the reaction of phenylacetylene with *p*-iodoanisole (Table 5, entry 2) was performed in the presence of the catalysts containing 5 mol% of grafted ligands. The conversion of aryl halide was 99 and 60 %, respectively, after 72 h of heating. Catalytic properties of materials **4b/SM** and **5b/SM** with respect to this reaction were also investigated using 5 mol% of grafted catalysts. For both materials, no coupling products were obtained after 16 h of reflux.

*General procedure for Huisgen cycloaddition.* A 8 ml glass vial was charged with alkyne (0.25 mmol), azide (0.25 mmol), triethylamine (34.7 μL, 0.25 mmol), **Cu/6b/SM/A** (4.3 mg, 1 mol%, calculated onto the grafted complex) and fresh distilled THF (1 mL) under Ar. A vial was closed with Teflon cap and the reaction mixture was stirred at 60 °C for 3 h. After cooling to room temperature, the organic phase was separated by centrifugation, and the solid catalyst was washed with THF (1 mL), methanol (1 mL x 2) and separated by centrifugation. The combined THF phases were evaporated to dryness under reduced pressure. The crude products were analysed by using <sup>1</sup>H NMR spectroscopy. Mesitylene was added as an internal standard. The spectral data of obtained products were in good agreement with the literature data.<sup>76-80</sup> The product yields are presented in Table 6.

A hot filtration test was performed for the reaction of phenylacetylene with *p*-nitrobenzyl azide (Table 6, entry 1). After 1h of heating, a half of the reaction mixture was taken by syringe equipped with a Acrodisc® syringe filter with Supor® membrane (pore size 10 μm) and introduced into a 8 ml glass vial under Ar. Then both reaction mixtures were stirred at reflux for additional 2 h and monitored by <sup>1</sup>H NMR spectroscopy. The results are shown in Figure S37.

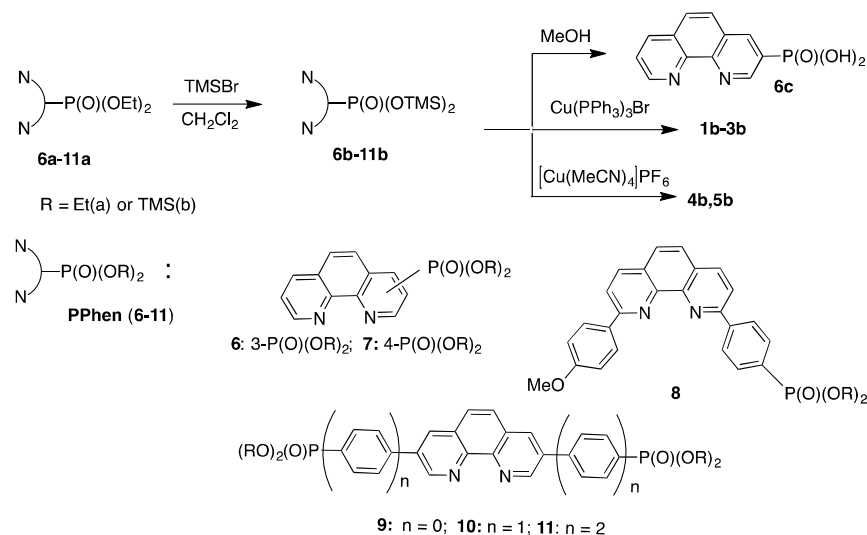
Recycling of **Cu/6b/SM/A** in the reaction of phenylacetylene with *p*-nitrobenzyl azide (Table 6, entry 1) was carried out. After washing, the catalyst was separated by centrifugation and dried under reduced pressure for 3 h and used in the next reaction cycle as reported above for the freshly prepared **Cu/6b/SM/A**. The product yields in 10 consecutive catalytic reactions are shown in Figure 5.

## Results and discussion

### Preparation of heterogenized catalysts

**Synthesis of copper(I) complexes bearing phosphonate anchoring groups.** Recently we reported the synthesis of air and moisture stable copper(I) complexes with (diethoxyphosphoryl)phenanthroline and triphenylphosphine ligands (**6a**, **7a** and **9a**) which catalyzed C–C and C–Het (Het = N, P) cross-coupling reactions.<sup>64,65,81</sup> These complexes could also be useful for the preparation of heterogeneous catalysts if the diethoxyphosphoryl substituent could be transformed into more reactive phosphonic acid or bis(trimethylsiloxy)phosphoryl groups (Scheme 1).<sup>53,82,83</sup>

Generally, the reaction of alkyl phosphonic acid diesters with TMSBr affords trimethylsilyl (TMS) diesters in high yields under mild conditions. However, when a solution of complex **1a** was reacted with TMSBr in CH<sub>2</sub>Cl<sub>2</sub> at room temperature a complicated mixture of products was obtained according to <sup>31</sup>P NMR analysis. Therefore, we decided to introduce the phosphorous anchoring group before the insertion of copper ions into chelators **6-11** (Scheme 2).



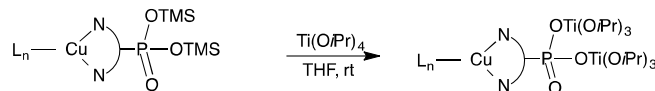
**Scheme 2.** Synthesis of molecular building blocks for the preparation of hybrid materials: silyl esters **6b-11b**, phosphonic acid **6c** and copper complexes **1b-5b**.

First, phosphonic acid **6c** was chosen as a model ligand. This compound was prepared in high yield (98%) by the treatment of diester **6a** with TMSBr followed by addition of MeOH. The acid **6c** was stable in air but hardly soluble in all organic solvents and aqueous media. All our attempts to prepare copper complexes reacting this ditopic chelator with tris(triphenylphosphine)copper(I) bromide (Cu(PPh<sub>3</sub>)<sub>3</sub>Br) and tetrakis(acetonitrile)copper(I) hexafluorophosphate ([Cu(CH<sub>3</sub>CN)<sub>4</sub>]PF<sub>6</sub>) were unsuccessful, probably due to a low selectivity of the complexation reaction under studied experimental conditions.

Next, TMS (1,10-phenanthrolyl)phosphonic acid diesters **6b-9b** were prepared by reacting compounds **6a-9a** with TMSBr in dichloromethane at room temperature when monitored by  $^1\text{H}$  NMR spectroscopy. These moisture sensitive compounds were obtained in quantitative yields and introduced in the next step without additional purification. Thus, after the reaction of **6a,7a** and **9a** with TMSBr run to completion, the volatiles were evaporated to dryness and the residue was reacted with  $\text{Cu}(\text{PPh}_3)_3\text{Br}$  in  $\text{CH}_2\text{Cl}_2$  to prepare heteroleptic complexes **1b-3b**. Alternatively, ligands **8b** and **9b** were treated with  $[\text{Cu}(\text{CH}_3\text{CN})_4]\text{PF}_6$  to yield homoleptic bis(phenanthroline) copper(I) complexes **5b** and **4b**, respectively. The progress of complexation was monitored by  $^{31}\text{P}$  NMR spectroscopy using the difference in the chemical shift of phosphorous nuclei of ligands **6b-9b** and corresponding complexes **1b-5b** ( $\Delta \delta$  1–2 ppm). After a full consumption of chelators, the volatiles were evaporated and the residues were introduced in the SG process (route A, Scheme 1) or anchored onto a mesoporous titania support prepared by us recently<sup>63</sup> (route B, Scheme 1).

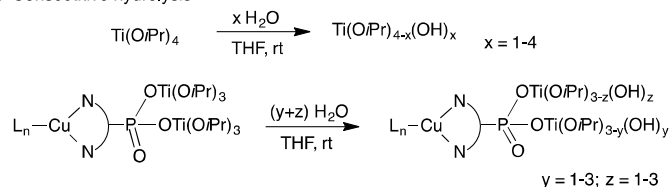
**Preparation of xerogels from copper(I) complexes 1b and 3b (route A, Scheme 1).** The first series of materials has been prepared from heteroleptic complexes **1b** and **3b** and  $\text{Ti}(\text{OiPr})_4$  according to the two-step SG process<sup>54,84</sup> as shown in Scheme 3. This one-pot co-condensation route provides a homogeneous distribution of functional groups within the hybrid solid. Copper complexes **1b** and **3b** were reacted with an excess of  $\text{Ti}(\text{OiPr})_4$  in THF to form titanium phosphonates (Step I). Subsequently, the hydrolysis, condensation and co-condensation reactions (Step II) were initiated by a dropwise addition of water diluted by THF to form a polymeric titania network containing covalently linked copper complexes. A gel which was formed immediately was aged at room temperature for two additional days. Then the solid was filtered, washed and dry at  $80^\circ\text{C}$  under reduced pressure for 24 h.

I. Step I: formation of titanium phosphonates

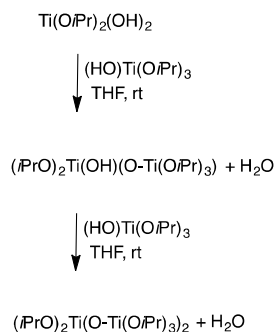


II. Step II: sol-gel processing in organic solvents

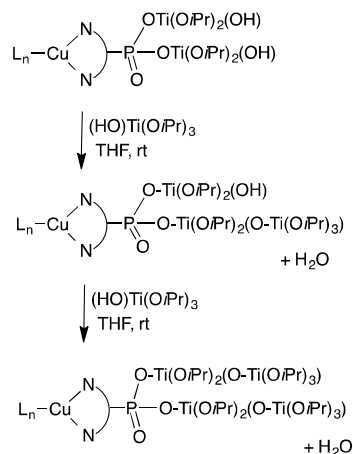
Ila. Consecutive hydrolysis



Ilb. Consecutive condensation reactions



Ilc. Consecutive co-condensation reactions



**Scheme 3.** Representative reactions involved in the preparation of hybrid xerogels **Cu/Pphen/SG**.

Five different materials **Cu/1b/SG/n** ( $n = 3, 10$ ) and **Cu/3b/SG/n** ( $n = 3, 10, 20$ ) were prepared varying the Ti:Cu molar ratio from 3 to 20 as indicated in Table 1 (see also the Supporting Information, Table S1). The xerogels were first characterized by elemental analysis, inductively coupled plasma optical emission spectroscopy (ICP-OES), thermogravimetric (TG) analysis, nitrogen adsorption–desorption at 77 K and FTIR spectroscopy. The molar ratio of components used for the material preparation, the chemical composition of xerogels and the

**Table 1.** Chemical composition and surface properties of xerogels **Cu/Pphen/SG**.

En-try	Xerogel <b>Cu/Pphen/SG</b>	<b>Cu/Pphen</b> : Ti(OiPr) <sub>4</sub> molar ratio in the synthesis	Chemical composition of the xerogel	<b>Pphen</b> : TiO <sub>2</sub> molar ratio in the xero- gel <sup>[a]</sup>	Cu : <b>Pphen</b> molar ratio in the xero- gel <sup>[b]</sup>	S <sub>BET</sub> [m <sup>2</sup> g <sup>-1</sup> ]
1	<b>1b/SG/10</b>	1:10	(Cu(PPh <sub>3</sub> )Br) <sub>0.34</sub> (C <sub>12</sub> H <sub>7</sub> N <sub>2</sub> O <sub>2</sub> P)(TiO <sub>2</sub> ) <sub>10</sub> (H <sub>2</sub> O) <sub>9.2</sub> (C <sub>3</sub> H <sub>7</sub> OH) <sub>3.5</sub>	1:10	0.34:1	10
2	<b>1b/SG/3</b>	1:3	(Cu(PPh <sub>3</sub> )Br) <sub>0.65</sub> (C <sub>12</sub> H <sub>7</sub> N <sub>2</sub> O <sub>2</sub> P)(TiO <sub>2</sub> ) <sub>3.6</sub> (H <sub>2</sub> O) <sub>8</sub> (C <sub>3</sub> H <sub>7</sub> OH) <sub>3.5</sub>	1:3.6	0.65:1	0
3	<b>3b/SG/20</b>	1:20	(Cu(PPh <sub>3</sub> )Br) <sub>0.38</sub> (C <sub>12</sub> H <sub>6</sub> N <sub>2</sub> O <sub>4</sub> P <sub>2</sub> )(TiO <sub>2</sub> ) <sub>18</sub> (H <sub>2</sub> O) <sub>40</sub> (C <sub>3</sub> H <sub>7</sub> OH) <sub>5</sub>	1:18	0.38:1	270
4	<b>3b/SG/10</b>	1:10	(Cu(PPh <sub>3</sub> )Br) <sub>0.40</sub> (C <sub>12</sub> H <sub>6</sub> N <sub>2</sub> O <sub>4</sub> P <sub>2</sub> )(TiO <sub>2</sub> ) <sub>10</sub> (H <sub>2</sub> O) <sub>20</sub> (C <sub>3</sub> H <sub>7</sub> OH) <sub>3.4</sub>	1:10	0.40:1	145
5	<b>3b/SG/3</b>	1:3	(Cu(PPh <sub>3</sub> )Br) <sub>0.40</sub> (C <sub>12</sub> H <sub>6</sub> N <sub>2</sub> O <sub>4</sub> P <sub>2</sub> )(TiO <sub>2</sub> ) <sub>2.6</sub> (H <sub>2</sub> O) <sub>10.7</sub> (C <sub>3</sub> H <sub>7</sub> OH) <sub>1.7</sub>	1:2.6	0.40:1	0

[a] The molar ratio was calculated from the P, N, Ti content determined by elemental analysis and ICP-OES. [b] The molar ratio was calculated from the Cu, P, N content determined by elemental analysis and ICP-OES. Expected Cu:**Pphen** ratio is 1:1.

calculated Brunauer–Emmett–Teller (BET) surface area are summarized in Table 1. Additional data on the material composition and their surface properties are presented in Tables S2, S3 and S12. The formulas of materials were derived from the content of six elements (C, H, N, P, Ti, Cu) assuming the presence of adsorbed water and isopropyl alcohol molecules that is obvious for xerogel samples. As seen in Table 1, the **Pphen**:TiO<sub>2</sub> molar ratio in materials was close to that of the starting compounds used in the reactions. In contrast, the content of copper atoms in all five **Cu/Pphen/SG** solids was lower than expected values. These data indicated that complexes **1b** and **3b** partially dissociated during the SG process. The successful incorporation of **Pphen** ligands in **Cu/Pphen/SG** xerogels was further confirmed by the analysis of filtrates obtained after the washing step. Combined liquid phases were evaporated to dryness and analysed by <sup>31</sup>P and <sup>1</sup>H NMR spectroscopies. The absence of signal sets corresponding to **phen** derivatives indicated that the incorporation of **Pphen** into the xerogels was quantitative. Thus, resulting hybrid materials contain the **Pphen** and Cu(**Pphen**)(PPh<sub>3</sub>)Br moieties linked to titania networks.

The presence of adsorbed water and isopropanol molecules in xerogels **1b/SG/n** and **3b/SG/n** was confirmed by TG analysis. In general, thermal patterns were similar for all studied samples. As an example, the TG curve of xerogel **3b/SG/20** is shown in Figure S22. A progressive weight loss comprised between 70 and 530 °C was observed. Accordingly, the separation of the initial loss of adsorbed solvents and the subsequent calcination of organic components was unclear. This thermal behaviour is a typical feature of titania xerogels in which solvent molecules are strongly chemisorbed on the titania surface.<sup>85–87</sup> Nevertheless, semiquantitative consideration of thermal data indicated that the loss of the initial weight for all samples was about 10–15% when the temperature was increased up to 200–250 °C, that



was about a half of maximal percentages of adsorbed solvents calculated from the chemical composition of the solids (Table 1). This difference can be explained by the presence of residual non-hydrolysed isopropoxy groups (*i*PrO–Ti) and non-condensed hydroxy groups (HO–Ti). These moieties are involved in the thermal reactions (condensation and decomposition) only when the temperature rises above 250 °C.

To prove the structure of organic moieties embedded into xerogels **1b/SG/n** and **3b/SG/n** and their covalent link to titania support, FTIR spectra of the solids were recorded (Figure 2, S23 and S24). Roughly, the spectra of all hybrid solids were remarkably similar in appearance. In Figure 2, FTIR spectrum of **3b/SG/3** is compared to those of the relevant ligand **9a** and the heteroleptic copper complex **3a**.

Bands having the greatest intensities are located between 900 and 1260 cm<sup>-1</sup> and associated with vibrations of the heteroaromatic moiety and its phosphonate substituent.<sup>88–90</sup> Notably, the shape of the **3b/SG/3** spectrum in this region is significantly different from those of ligand **9a** and complex **3a** that points to the covalent bonding of the phosphonate group to the titania matrix. In particular, a strong broad band in 950–1150 cm<sup>-1</sup> region observed for material **3b/SG/3** is commonly associated with Metal–O–P stretching vibrations.<sup>91,92</sup> Moreover, characteristic vibrations of **phen** heterocycle are also observed in two frequency regions, namely 700–900 and 1350–1600 cm<sup>-1</sup> in all three spectra. Despite the overlapping of **Pphen** and PPh<sub>3</sub> vibration bands, the latter can be identified owing to the presence of a relatively strong band at 1430 cm<sup>-1</sup> typical of the vibration of the phenyl ring directly attached to a phosphorous atom and a medium band at 690 cm<sup>-1</sup>.<sup>93</sup> The O–H stretching bands at 3500–3700 cm<sup>-1</sup>, associated with Ti–OH groups and adsorbed water, and weak bands in 2900–3100 cm<sup>-1</sup> region, characteristic of the aromatic and aliphatic C–H bonds are also present in the spectrum of **3b/SG/3**.

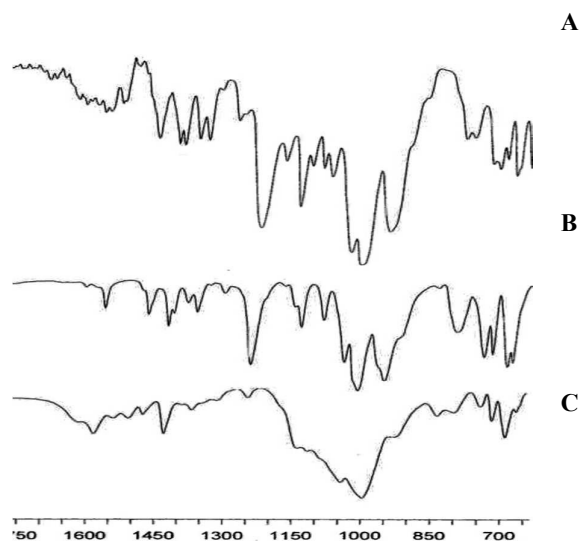


**Figure 2.** FTIR spectra of **9a**(A), **3a**(B) and **3b/SG/3**(C).

It has to be noted, that stretching vibrations of the phosphonate group in 950–1250 cm<sup>-1</sup> region were commonly used for disclosing of the binding mode of phosphonate molecules to a titania network.<sup>83,91,92</sup> However, recently Blockhuys et al. have demonstrated that FTIR spectroscopy is not well suited for the investigation of the bonding mode in hybrid materials because P–O and P=O stretches are also depend on hydrogen bonding.<sup>94</sup> For solids **1b/SG/n** and **3b/SG/n**, this analysis is even more complicated due to the overlapping these stretches with vibrations of the heterocyclic moiety. For example, a weak band at approximately 1250

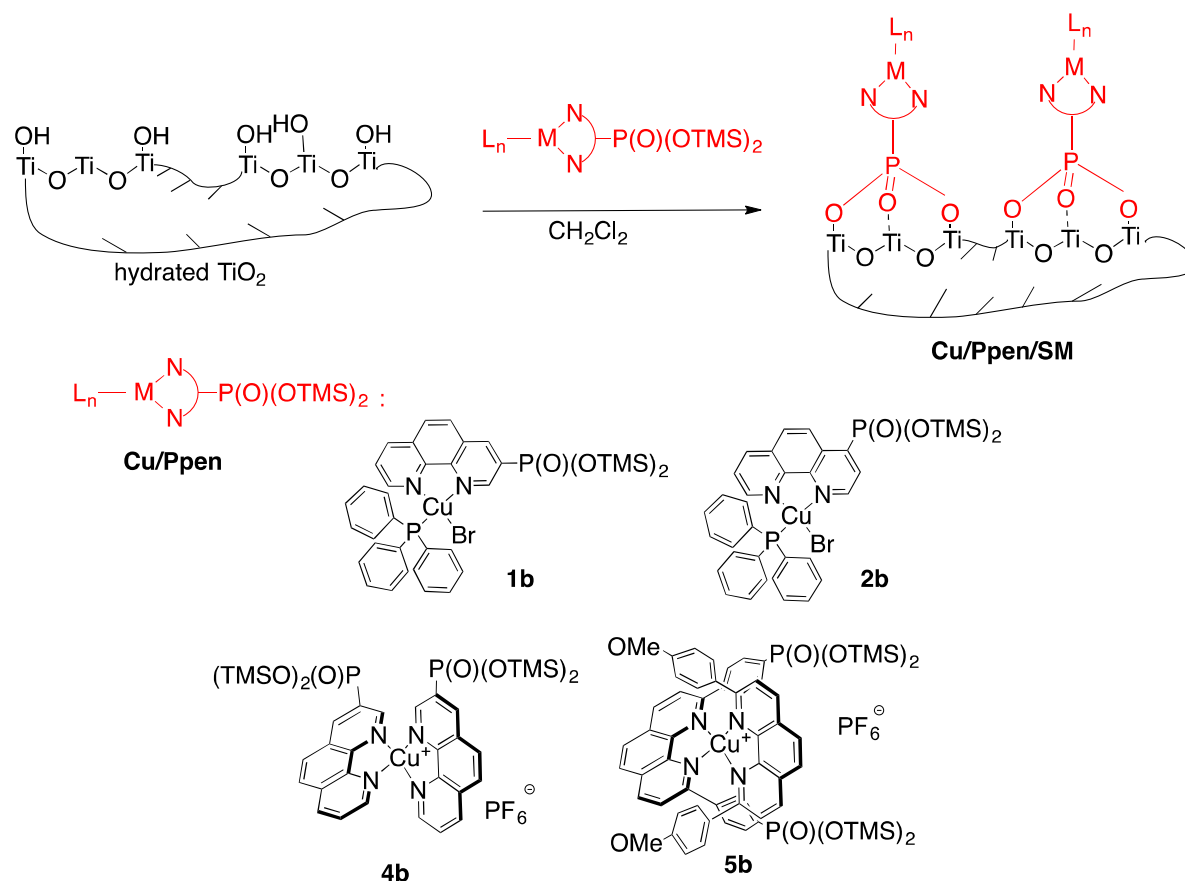
$\text{cm}^{-1}$  can be assigned to vibration of the uncoordinated P=O group or the heteroaromatic fragment.

Powder X-ray diffraction measurements indicate that all materials are non-crystalline.

The porosity of xerogels **1b/SG/n** and **3b/SG/n** was examined by nitrogen adsorption-desorption at 77 K. Interestingly, BET surface areas were dependent on the number of phosphonate groups at **phen** ligands and the amount of  $\text{Ti}(\text{O}i\text{Pr})_4$  employed for the incorporation of complexes. Solids **1b/SG/3** and **1b/SG/10** containing monophosphonate residues were non-porous. Material **3b/SG/20** prepared from the copper complex with (**phen**)diphosphonate **3b** and 20 equiv of  $\text{Ti}(\text{O}i\text{Pr})_4$  exhibited a micro- and mesoporosity and a remarkable specific surface area (BET surface area of  $270 \text{ m}^2 \text{ g}^{-1}$ ). However, in a series of xerogels **3b/SG/20–3b/SG/3**, this value dropped drastically (Table 1 and S12) with the decrease of titania percentage that is a serious drawback for their applications in catalysis.

To increase porosity of hybrid materials and the content of copper ions, another strategy of immobilization was investigated. The complexes were grafted onto a surface of pre-formed  $\text{TiO}_2$ .

**Surface modification of  $\text{TiO}_2$  by copper(I) complexes (route B, Scheme 1).** Recently we have reported the preparation of non-ordered mesoporous titania exhibited a remarkable specific surface area of  $580\text{--}650 \text{ m}^2 \text{ g}^{-1}$  and pore volumes of  $0.5\text{--}1.2 \text{ cm}^3 \text{ g}^{-1}$ .<sup>63</sup> This cost-effective hydrated  $\text{TiO}_2$  is readily available according to a template-free SG process and promising for the preparation of heterogeneous catalysts. A surface modification of  $\text{TiO}_2$  by phosphonates is shown in Scheme 4. Silyl phosphonate diesters are reacted with a pre-formed titania support bearing reactive hydroxy groups. Accordingly, water is no more needed for the immobilization and the SM reaction can be performed in all organic solvents in which the targeted complexes can be dissolved. Copper complexes **1b** and **2b** are readily soluble in chlorinated solvents and we chose weakly coordinating  $\text{CH}_2\text{Cl}_2$  as a reaction medium to prevent the dissociation of copper complexes.



**Scheme 4.** Schematic representation of grafting of copper(I) complexes with **Pphen-Si** ligands onto a titania support.

Complexes **1b** and **2b** smoothly reacted with TiO<sub>2</sub> powders in CH<sub>2</sub>Cl<sub>2</sub> at room temperature. Hybrid solids **Cu/Pphen/SM** were filtrated after 48 h of stirring, dried at 80 °C under reduced pressure and examined by elemental and ICP-OES analyses (Tables 2, S4-S6).

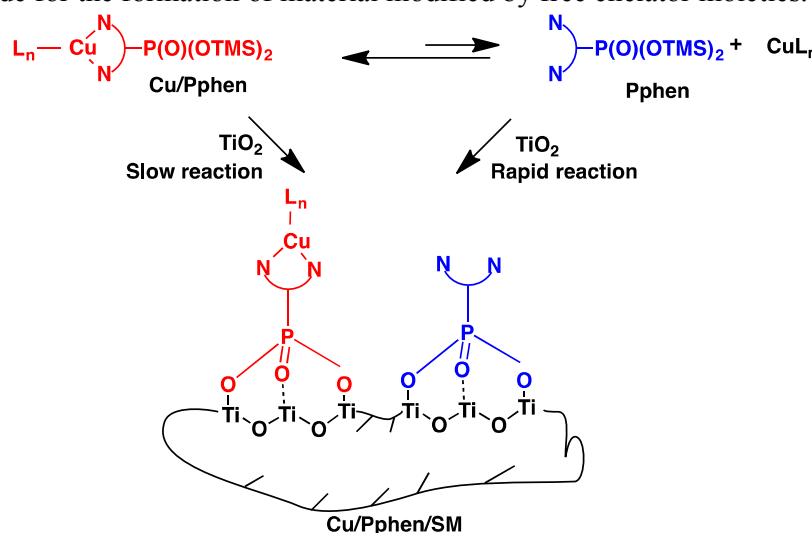
**Table 2.** Chemical composition and surface properties of xerogels **Cu/Pphen/SM**.

En-try	Material	<b>Cu/Pphen</b> : TiO <sub>2</sub> <sup>[a]</sup> molar ratio in the synthesis	Chemical composition of the xerogel	<b>Pphen</b> : TiO <sub>2</sub> molar ratio in the solid <sup>[b]</sup>	<b>Cu</b> : <b>Pphen</b> molar ratio in the solid <sup>[c]</sup>	S <sub>BET</sub> [m <sup>2</sup> g <sup>-1</sup> ]
1	<b>1b/SM</b>	1:10	(Cu(PPh <sub>3</sub> )Br) <sub>0.18</sub> (C <sub>12</sub> H <sub>7</sub> N <sub>2</sub> O <sub>2</sub> P)(TiO <sub>2</sub> ) <sub>9.7</sub> (H <sub>2</sub> O) <sub>11</sub> (C <sub>3</sub> H <sub>7</sub> OH) <sub>0.8</sub>	1:9.7	0.18:1 <sup>[d]</sup>	317
2	<b>2b/SM</b>	1:10	(Cu(PPh <sub>3</sub> )Br) <sub>0.14</sub> (C <sub>12</sub> H <sub>7</sub> N <sub>2</sub> O <sub>2</sub> P)(TiO <sub>2</sub> ) <sub>9.5</sub> (H <sub>2</sub> O) <sub>11</sub> (C <sub>3</sub> H <sub>7</sub> OH)	1:9.5	0.14:1 <sup>[d]</sup>	nd <sup>[e]</sup>
3	<b>4b/SM</b>	1:10	Cu(C <sub>12</sub> H <sub>7</sub> N <sub>2</sub> O <sub>2</sub> P) <sub>2</sub> PF <sub>6</sub> (TiO <sub>2</sub> ) <sub>11</sub> (H <sub>2</sub> O) <sub>18</sub> (C <sub>3</sub> H <sub>7</sub> OH) <sub>0.6</sub>	1:11	1:2 <sup>[f]</sup>	290
4	<b>5b/SM</b>	1:20	Cu(C <sub>25</sub> H <sub>17</sub> N <sub>2</sub> O <sub>2</sub> P) <sub>2</sub> PF <sub>6</sub> (TiO <sub>2</sub> ) <sub>19</sub> (H <sub>2</sub> O) <sub>22</sub>	1:19	1:2 <sup>[f]</sup>	270

[a] A TiO<sub>2</sub> powder with BET surface areas of 650 m<sup>2</sup> g<sup>-1</sup> was prepared according to the sol-gel process. [b] The molar ratio was calculated from the P, N, Ti content determined by elemental analysis and ICP-OES. [c] The molar ratio was calculated from the Cu, P, N content determined by elemental analysis and ICP-OES. [d] Expected Cu:**Pphen** ratio is 1:1. [e] Not determined. [f] Expected Cu:**Pphen** ratio is 1:2.

The Ti:N and Ti:P molar ratios indicated quantitative grafting of **Pphen** ligands.

Surprisingly, Cu:Pphen molar ratio was low in both materials as it was previously observed for Cu/Pphen/SG xerogels. Thus, once again resulting hybrid materials contain Pphen and Cu(Pphen)(PPh<sub>3</sub>)Br moieties linked to the titania support. These results can be explained by kinetic lability of heteroleptic copper complexes (Scheme 5). In fact, according to <sup>1</sup>H and <sup>31</sup>P NMR studies of chelates **1** and **2** only one major species exists in CDCl<sub>3</sub> solution for each of these complexes (Figures S1-S4, S16 and S17). In these mononuclear species, phen moieties are coordinated to copper centres by two nitrogen atoms and a rapid exchange of Pphen ligands is highly probable.<sup>65</sup> For example, line broadening in the room temperature <sup>1</sup>H NMR spectrum of complex **1b** could be caused by the ligand exchange (Figure S16). The immobilization of the Pphen ligand which could be present in solution in a low concentration should proceed more rapidly than the incorporation of bulky heteroleptic complex Cu/Pphen. Accordingly, the complexation equilibrium could be moved to the non-coordinated ligand that should provide for the formation of material modified by free chelator moieties.



**Scheme 5.** Schematic representation of Cu/Pphen complexes grafting on titania support.

To check this hypothesis, kinetically more stable<sup>65</sup> homoleptic complexes **4b** and **5b** were grafted onto TiO<sub>2</sub> surface (Table 2). As evidenced by Cu:Ti, Cu:P, Cu:N molar ratios obtained for these materials (Tables S6), the immobilization was successful in both cases. FTIR spectra of solids **4b/SM** and **5b/SM** shown in Figures S25-S26 corroborated the proposed molecular structure of materials.

Porosity of Cu/Pphen/SM materials was studied by N<sub>2</sub> sorption measurements (Table 2 and S12). The shapes of all isotherms were similar and resembled to that of the non-modified titania support. In contrast, BET surface areas of hybrid materials were smaller compared to that of the as-synthesized TiO<sub>2</sub>. This indicates the successful grafting of complexes onto a surface of mesopores.

Being unable to overcome the dissociation of heteroleptic copper complexes, we have turned to a stepwise strategy for the preparation of heterogeneous catalysts. This method involves the incorporation of free Pphen ligands into a titania support followed by their complexation with copper ions.

**Immobilization of Pphen-Si ligands followed by the insertion of copper ions (routes C and D, Scheme 1).** The first series of materials have been prepared according to the SG process as described above for copper complexes, with the only difference that Pphen-Si chelators were used as molecular precursors (Scheme 1 and 3). Materials **6b/SG** and **9b/SG** was characterized by elemental analysis, ICP-OES, nitrogen adsorption-desorption at 77 K (Table 3, S7 and S8, entries 1 and 2). As seen from these data, Ti:N and Ti:P molar ratios are

very close to theoretical values. However, both solids display a pretty low BET surface area of 215 and 160 m<sup>2</sup> g<sup>-1</sup>, respectively. Our attempt to increase a xerogel porosity by using bulkier ligands in which the **phen** moiety and phosphonate substituents were separated by phenyl spacers (compounds **10b** and **11b**, Figure 1) have met with only a partial success (Table 3, entries 3 and 4). The BET surface areas of xerogels **10b/SG** and **11b/SG** were 270 and 300 m<sup>2</sup> g<sup>-1</sup>, respectively, even when Ti(OiPr)<sub>4</sub> was used in a large excess (20 equiv).

**Table 3.** Chemical composition and surface properties of xerogels **Pphen/SG**.

En-try	Material <b>Pphen/SG</b>	<b>Pphen</b> : Ti(OiPr) <sub>4</sub> molar ratio in the synthesis	Chemical composition of the material	<b>Pphen</b> :TiO <sub>2</sub> molar ratio in the solid <sup>[a]</sup>	S <sub>BET</sub> [m <sup>2</sup> g <sup>-1</sup> ]
1	<b>6b/SG</b>	1:10	(C <sub>12</sub> H <sub>7</sub> N <sub>2</sub> O <sub>2</sub> P)(TiO <sub>2</sub> ) <sub>9.2</sub> (H <sub>2</sub> O) <sub>12</sub> (C <sub>3</sub> H <sub>7</sub> OH) <sub>1.9</sub>	1:9.2	215
2	<b>9b/SG</b>	1:10	(C <sub>12</sub> H <sub>6</sub> N <sub>2</sub> O <sub>4</sub> P <sub>2</sub> )(TiO <sub>2</sub> ) <sub>10</sub> (H <sub>2</sub> O) <sub>19.5</sub> (C <sub>3</sub> H <sub>7</sub> OH) <sub>1.2</sub>	1:10	160
3	<b>10b/SG</b>	1:20	(C <sub>24</sub> H <sub>14</sub> N <sub>2</sub> O <sub>4</sub> P <sub>2</sub> )(TiO <sub>2</sub> ) <sub>17.9</sub> (H <sub>2</sub> O) <sub>27</sub> (C <sub>3</sub> H <sub>7</sub> OH) <sub>3.5</sub>	1:17.9	270
4	<b>11b/SG</b>	1:20	(C <sub>36</sub> H <sub>22</sub> N <sub>2</sub> O <sub>4</sub> P <sub>2</sub> )(TiO <sub>2</sub> ) <sub>18.8</sub> (H <sub>2</sub> O) <sub>37</sub> (C <sub>3</sub> H <sub>7</sub> OH) <sub>0.9</sub>	1:18.8	300

[a] The molar ratio was calculated from the P, N, Ti content determined by elemental analysis and ICP-OES.

Next, silyl phosphonate **1b** was grafted onto a surface of TiO<sub>2</sub> in CH<sub>2</sub>Cl<sub>2</sub> at room temperature as described above for copper complexes. As expected, the reaction proceeds quantitatively yielding porous hybrid material **6b/SM** which was firstly characterized by elemental analysis (Table S7 and S8), EDX spectrometry, FTIR (Figure S31) and <sup>31</sup>P MAS NMR spectroscopies. In particular, the <sup>31</sup>P MAS NMR spectrum shows a broad signal typical of non-ordered solids based on titania at about 5 ppm (Figure 3). The <sup>31</sup>P chemical shifts in amorphous titania phosphates were reported between -21 and -4 ppm.<sup>95</sup> Thus, the cleavage of C–P bond was not observed under these experimental conditions and phosphorous atoms in the material are bonded to the **phen** scaffold and the three oxygen atoms. Phosphorous signals of layered titanium phosphonates are obviously observed at -4 ppm as sharp signals<sup>95</sup> that doesn't match with our spectrum. These data indicate that **phen** moieties are separated one from others onto the titania surface. The experimental spectrum of **6b/SM** was deconvoluted as shown in Figure 3. According to this analysis, the experimentally observed signal is a superposition of three sharp resonances originated from non-equivalent phosphorous sites. Based on relative positions of three signals in <sup>31</sup>P MAS NMR spectra of titania-supported phenylphosphonic acid,<sup>83,94,96</sup> the major signal (δ 4.8 ppm, 80%) was attributed to the phosphonate group exhibited a tridentate binding mode and the two other signals were assigned to mono- (δ -2.7 ppm) and bidentate (δ 7.2 ppm) phosphonate groups.

Interestingly, qualitative EDX-STEM analysis of this material indicated the presence of Br among with the other expected elements (Figures S34 and S35). We have assumed that the **phen** ligand was partially protonated by traces of hydrobromic acid when it was reacted with TMSBr.



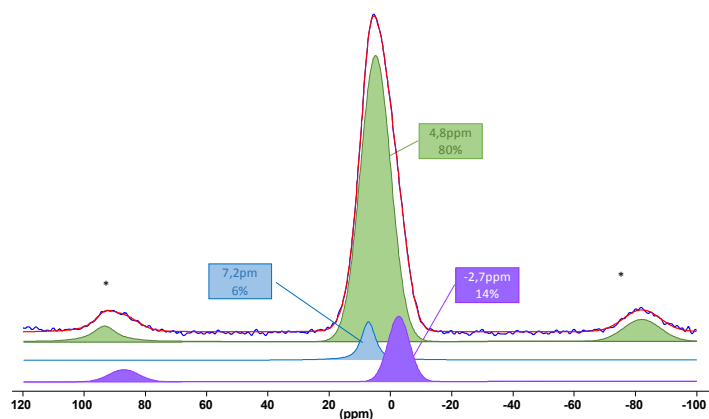


**Figure 3.** Experimental (blue) and simulated (red)  $^{31}\text{P}$  MAS NMR spectrum of material **6b/SM**. The stars indicate spinning sidebands.

Nitrogen adsorption–desorption isotherms of solid **6b/SM** and bare  $\text{TiO}_2$  support are presented in Figure 4A and pore size distributions for these materials are shown in Figure 4B. The features of two isotherms are very similar. They demonstrate a gradual increase in the adsorbed nitrogen volume in function of the relative pressure making a hysteresis loop. The morphology of the curves can be considered as a combination of type II and type IV isotherms that are typical for non-ordered porous solids containing both mesopores and macropores with a large distribution of the pore size. The BET surface area was lowered from 650 to 366  $\text{m}^2 \text{g}^{-1}$  after grafting the ligand **6b**. This surface modification has also caused a significant decrease in the amount of small mesopores in  $\text{TiO}_2$  (Figure 4B).

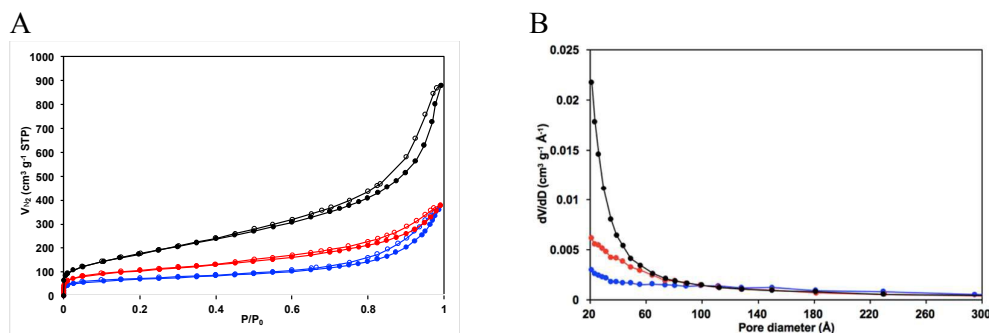


**Figure 4.** Nitrogen adsorption–desorption studies: isotherms for as-synthesized hydrated  $\text{TiO}_2$  (black), solid **6b/SM** (red) and **Cu/6b/SM/A** (blue) (A); pore size distribution (BJH calculations) for as synthesized  $\text{TiO}_2$  (black), **6b/SM** (red) and **Cu/6b/SM/A** (blue) (B).

As can be seen from Tables 3 and S12, porosity of material **6b/SM** was superior to those of hybrid materials **Pphen/SG** prepared by the SG method. In addition, in this material, chelator moieties are located on the titania surface and more accessible for reactant molecules than in **Pphen/SG** materials in which the ligands are buried inside the solids. Thus, **6b/SM** material was chosen for the preparation of the heterogeneous catalyst. The insertion of copper ions was performed by stirring this solid with various copper(I) complexes in  $\text{CH}_2\text{Cl}_2$  at room temperature (Table 4). The chelation was sluggish due to a strong steric hindrances induced

by the solid support and/or the partial protonation of the titania-supported **pphen** ligand. First, solid **6b/SM** was reacted with 1.1 equiv of  $\text{Cu}(\text{PPh}_3)_3\text{Br}$  which we previously used to prepare related **Pphen** complexes **1-3** under homogeneous conditions. According to the elemental analysis and ICP-OES data for resulting materials,  $\text{Cu}:\text{Pphen}$  molar ratio was only 0.16 (entry 1). When  $\text{Cu}(\text{PPh}_3)_3\text{Br}$  amount was increased up to 2.6 equiv, the complexation of 29% of the grafted ligand was achieved (entry 2). Fortunately,  $[\text{Cu}(\text{MeCN})_4]\text{PF}_6$  complex bearing less bulky ligands was more reactive and gave the targeted material **Cu/6b/SM/A** (entry 3). Empirical formula of this material was derived from its elemental analysis (Table S10 and S11). In addition, the presence of fluor in the powder was confirmed by EDX-TEM analysis (Figure S36). It has to be also noted, that brom was not found in the studied sample. These data are in agreement with our hypothesis that the titania-supported **pphen** ligand is partially protonated in the material **6b/SM**. Accordingly, bromine anion is no more present in the solid after the complexation reaction.

**Table 4.** Insertion of copper(I) ions into material **6b/SM**.

Entry	Solid	Copper complex (equiv of grafted <b>6b</b> )	$\text{Cu}:\text{6b}$ molar ratio <sup>[a]</sup>	$S_{\text{BET}}$ [ $\text{m}^2\text{g}^{-1}$ ]
1	<b>Cu/6b/SM/P1</b>	$\text{Cu}(\text{PPh}_3)_3\text{Br}$ (1.1)	0.16:1	nd <sup>[b]</sup>
2	<b>Cu/6b/SM/P2</b>	$\text{Cu}(\text{PPh}_3)_3\text{Br}$ (2.6)	0.29:1	nd <sup>[b]</sup>
3	<b>Cu/6b/SM/A</b>	$[\text{Cu}(\text{MeCN})_4]\text{PF}_6$ (2.6)	1:1	243

[a] The molar ratio was calculated from the Cu, P, N content determined by elemental analysis and ICP-OES.

[b] Not determined.

Nitrogen adsorption–desorption isotherm of **Cu/6b/SM/A** at 77 K is presented in Figure 4A and compared to those of bare titania support and starting material **6b/SM**. Upon the stepwise derivatization of  $\text{TiO}_2$ , no change in the shape of isotherms was observed, whereas a marked decrease in the BET surface area (from 650 to  $246\text{ m}^2\text{g}^{-1}$ , Table S12) and pore volume (from  $1.36$  to  $0.55\text{ cm}^3\text{g}^{-1}$ , Table S12) was noted, which is consistent with the presence of a significant amount of grafted complex on the surface.

The morphology of solids **6b/SM** and **Cu/6b/SM/A** was studied by SEM and TEM microphotographies and compared to that of the bare  $\text{TiO}_2$  support. SEM images are shown in Figure 5. As-synthesized hydrated  $\text{TiO}_2$  is composed of the strongly aggregated nanoparticles displaying a similar shapes and quite narrow distribution of the grain size. As seen in Figure 5, grafting of the **Pphen** ligand (material **6b/SM**) and the following insertion of copper(I) ions (material **Cu/6b/SM/A**) do not influence on the morphology of solids. TEM images of **6b/SM** and **Cu/6b/SM/A** are shown in Figure S33. The mesoporous nanospheroids with a diameter ranging from 5 to 20 nm are irregularly distributed in the space and separated by large widths of hundreds of nanometres. Calculated external specific surface area for non-aggregated anatase nanoparticles of this size is in the range of  $75\text{--}300\text{ m}^2\text{g}^{-1}$  that evidences the presence of interior mesopores in at least bare  $\text{TiO}_2$  ( $S_{\text{BET}} = 650\text{ m}^2\text{g}^{-1}$ ). This morphology perfectly fits the catalytic application providing the accessibility of catalytic sites and a mass transfer of reagents and products through large canals separating the nanoparticles. Powder X-ray measurements demonstrate that these samples are non-crystalline (Figure S37).

A

B

C

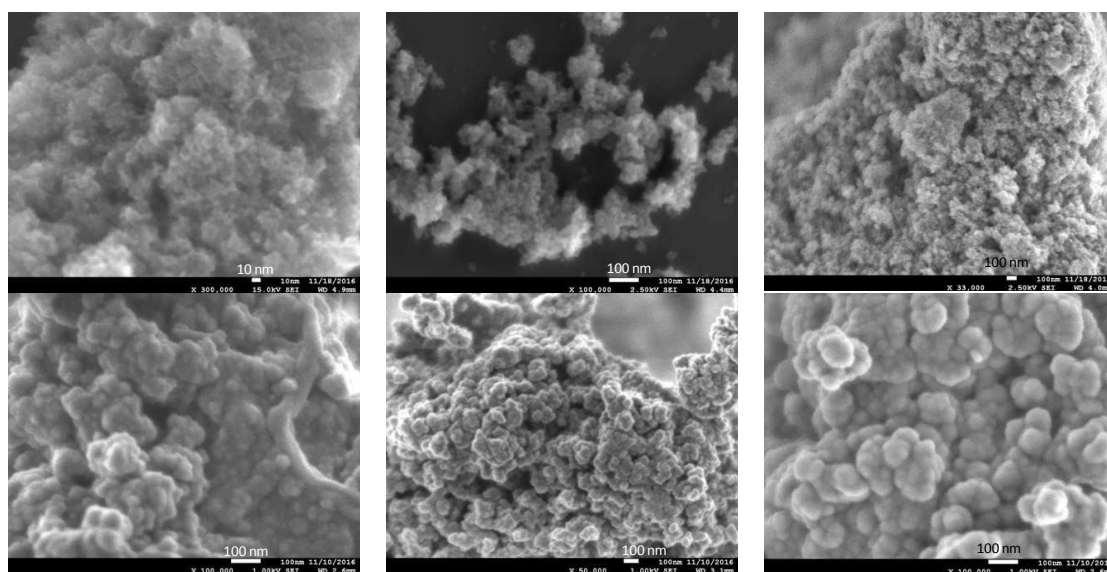


**Figure 5.** SEM microphotographs of bare hydrated  $\text{TiO}_2$  (A), solid **6b/SM** (B) and material **Cu/6b/SM/A** (C). Upper microphotographs of each series were obtained from powders deposited on a silicon wafer as ethanol suspensions. Bottom images were observed using samples prepared by the dispersion the materials on a conductive carbon tape and carbon coating (8 nm).

All **Cu/Pphen/SG** and **Cu/Pphen/SM** materials except **5b/SM** change their brown colour to green-blue being exposure to air during a few weeks. Oxidation of copper(I) ions was assumed and proved by EPR spectroscopy and the diffuse reflectance spectroscopy. As a representative example, EPR spectrum of **Cu/6b/SM/A** stored in the air is presented in Figure S38. The spectrum recorded in X-band frequencies at 100 K shows a broad line in the region of 2500–3600 G due to an intermolecular spin exchange caused by spin coupling between paramagnetic copper(II) centres located in close proximity. As a result, the anisotropic  $g_i$  values cannot be determined by simulation experiments due to the broad linewidth that precluded any studies of a copper ion environment in the solid state. We also observed a very large and weak band in the region of 700–950 nm in the diffuse reflectance spectrum of **Cu/6b/SM/A** due to d-d electron transitions in copper(II) complexes.<sup>97,98</sup> However, a weak intensity of this band and its broadness also excluded any conclusions on the copper(II) ion environment (Figure S39).

## Catalytic Reactions

**Sonogashira coupling.** Catalytic cross-coupling reaction of aryl halide with terminal acetylenes is a well-known and useful method in organic synthesis which is frequently employed for the synthesis of biologically active molecules, heterocycles, natural products, or polymers.<sup>99,100</sup> Commonly, this reaction is performed in anhydrous solvents in the presence of tertiary amines, palladium catalysts and with copper salts as co-catalysts. Palladium-free conditions were also widely explored<sup>99,101-103</sup> but heterogenized copper complexes are still limited by a few examples.<sup>47,104-107</sup>

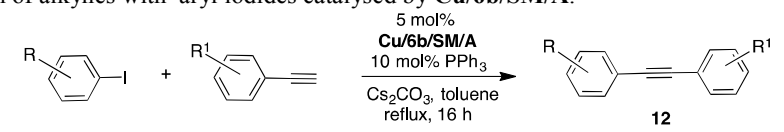
In the preliminary experiment, a model reaction of *p*-iodoanisole with phenylacetylene in toluene at 110 °C was performed in the presence of cesium carbonate and 5 mol% of **Cu/6b/SM/A** (Table 5, entry 1). The reaction proceeded slowly yielding the product of C–C coupling in 27 and 77 % yield after 16 and 72 h, respectively. When 10 mol% of  $\text{PPh}_3$  was added, the reaction afforded the target product **12** in 98% yield after 16 h of reflux. The reaction performed in the dark proceeds as well as in the daylight. This indicates that any

photocatalytic processes were not observed under studied conditions. To determine whether a non-supported copper catalyst could catalyse the reaction, a hot filtration test was performed (Figure S40). The filtered solution didn't show any catalytic activity that testified a heterogeneous catalytic process. The positive role of PPh<sub>3</sub> in this heterogeneous reaction can stem from its influence on the structure of intermediate complexes involving in the catalytic cycle or its ability to reduce inactive Cu(II) complexes to copper(I) chelates.<sup>108</sup>

To prove that grafted phenanthroline complexes are true catalytic centres and clarify the role of **pphen** ligand, titania-supported Cu(MeCN)<sub>4</sub>PF<sub>6</sub> was prepared by the impregnation of TiO<sub>2</sub> powder in CH<sub>2</sub>Cl<sub>2</sub> solution of this complex at room temperature. This material and non-modified titanium support didn't promote the studied reaction indicating that titania-supported **Cu/Pphen** complexes are involved in the catalytic cycle.

Next, the reaction scope was explored. Coupling products **12** were obtained in near-quantitative yield starting from aryl iodides with electron-donating or electron-withdrawing

**Table 5.** Reaction of alkynes with aryl iodides catalysed by **Cu/6b/SM/A**.<sup>[a]</sup>



5 mol%  
**Cu/6b/SM/A**  
10 mol% PPh<sub>3</sub>  
Cs<sub>2</sub>CO<sub>3</sub>, toluene  
reflux, 16 h

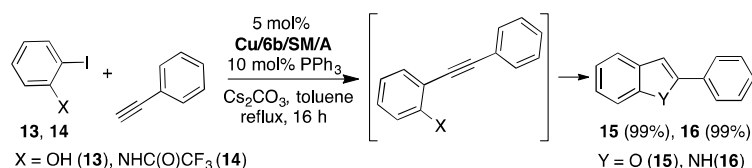
**12**

Entry	Alkyne	Aryl halide	Product	Yield <sup>[b]</sup> [%]
1 <sup>[c]</sup>				27 <sup>[d]</sup>
2(1st cycle)				99
3(2nd cycle)				98
4(3d cycle)				99
5(4th cycle)				99
6(5th cycle)				99
7				99
8				99
9				99
10				99
11				99
12				99
13				99
14				99
15				99
16				99

[a] Reaction conditions: 0.75 mmol of the alkyne, 0.5 mmol of the aryl halide, 1 mmol of Cs<sub>2</sub>CO<sub>3</sub>, 5 mol% **Cu/6b/SM/A** (calculated onto the grafted complex) and 10 mol% of PPh<sub>3</sub> were refluxed in toluene (2 mL) under Ar. [b] The yield was determined by <sup>1</sup>H NMR spectroscopy of the crude product. [c] Reaction was performed without PPh<sub>3</sub>. [d] 77% conversion of the aryl halide was observed after 72 h.

groups including sterically bulky *o*-isomers. Phenylacetylene can also be replaced by different aliphatic or aromatic alkynes without any loss of selectivity and product yield (entries 11-16).

After the reaction runs to completion, the catalyst can be recovered by centrifugation, washing with MeOH and subsequent drying at 80 °C under reduced pressure. The catalytic performance of the recovered solid was explored in the reaction of *p*-iodoanisole with phenylacetylene. The catalyst was reused in five consecutive cycles retaining completely the selectivity and the product yield (entries 2-6). The recycled solids were also introduced in the reactions with different aryl iodides (entries 7-10) and shown the same catalytic efficiency as catalyst **Cu/6b/SM/A**. When *o*-iodophenol (**13**) or *o*-iodo(trifluoroacetyl)aniline (**14**) were reacted with phenylacetylene, cascade catalytic reactions involving the Sonogashira coupling and the addition of N–H or O–H bonds to the triple bond are observed to yield benzofuran **15** and indole **16** (Scheme 6). The cyclization products were obtained in quantitative yield.



**Scheme 6.** Cascade reactions of iodides **13** and **14** with phenylacetylene.

It's worthy to note that materials **3b/SG/10**, **3b/SG/20**, **1b/SM** and **2b/SM** based on copper complexes with one **phen** ligand also catalyse the reaction of phenylacetylene with *p*-iodoanisole. However, they are less convenient in practice due to a smaller number of catalytic centres as compared to **Cu/6b/SM/A**. In contrast, **4b/SM** and **5b/SM** prepared by grafting bis(**Pphen**)copper complexes **4b** and **5b** were inactive like their counterpart **4a** and **5a**, respectively, which were studied under homogeneous conditions. These results are in accordance with previous reports<sup>81</sup> and can be explained by a slow dissociation kinetics of copper complexes bearing two **phen** ligands.

**Huisgen 1,3-dipolar cycloaddition.** Copper-catalysed alkyne-azide cycloaddition is a novel synthetic paradigm having a remarkable practical and ecological impact and widely employing in the synthesis of many functional molecules including pharmaceuticals, dyes, sensors, and bioconjugates.<sup>109-116</sup> This reaction allows to deliver sophisticated molecules or libraries of substituted 1,2,3-triazoles due to its selectivity, excellent functional compatibility, reliability and simplicity of experimental conditions. However, the separation of targeted molecules from

resting copper by-products is still challenging and has a primordial importance for further developing of this synthetic method.<sup>33,35,41,117-120</sup> In this regard, we have explored the alkyne-azide cycloaddition in the presence of material **Cu/6b/SM/A** (Table 6). First, the reaction conditions were optimized using the reaction of phenylacetylene with *p*-nitrobenzyl azide as a model reaction. The solvent was found to be a key parameter influencing the reaction rate. The cycloaddition product was not detected when the reaction was run in toluene or dichloromethane. Polar coordinating solvents like THF or DMF were required to obtain a complete conversion to 1,2,3-triazole and in THF, the reaction was rapid. When it was performed at 60 °C in the presence of triethylamine and 5 mol% of **Cu/6b/SM/A**, the product was isolated in near-quantitative yield after 1 h of stirring (Table 8, entry 1). Complete conversion was also achieved employing 1 mol% of the catalyst although the reaction time should be increased up to 3 h (entry 2). Noteworthy, the reaction was not observed under studied conditions without the catalyst and in presence of the non-modified TiO<sub>2</sub> powder. A hot filtration test revealed that the cycloaddition proceeds as a heterogeneous process even



being performed in coordinating THF solvent and in the presence of triethylamine that is a strong ligand for copper ions (Figure S41).

**Table 6.** Huisgen cycloaddition catalysed by **Cu/6b/SM/A**.<sup>[a]</sup>

Entry	Alkyne, R <sub>1</sub>	Azide	Product	Yield <sup>[b]</sup> [%]
1 <sup>[c]</sup>	H			99
2	H			99
3	H			99
4	H			95
5	Me			99
6	<i>t</i> Bu			99
7	CO <sub>2</sub> Me			96
8	CN			92

[a] Reaction conditions: 0.25 mmol of the alkyne, 0.25 mmol of the azide, 0.25 mmol of NEt<sub>3</sub>, 1 mol% of **Cu/6b/SM/A** (calculated onto the grafted complex) in THF (1 mL) at 60 °C under Ar. [b] Isolated yields. [c] The reaction was performed with 5 mol% of **Cu/6b/SM/A** (calculated onto the grafted complex) during 1 h.

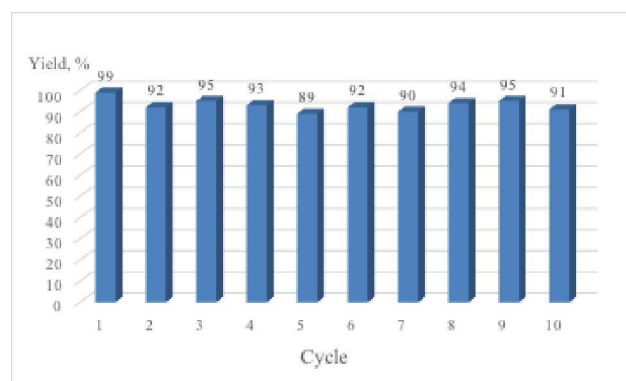


**Figure 6.** Recycling of **Cu/6b/SM/A** in the Huisgen cycloaddition of phenylacetylene with *p*-nitrobenzyl azide (Table 8, entry 1).

The reaction was successful and run without complications with azides bearing benzyl and even alkyl residues (entries 3-5). The aromatic alkynes gave high yields of click products independently of whether electron-donor or electron-withdrawing substituents were present in the aromatic ring (entries 5-8).

The catalyst recovering and refining was straightforward. After reaction completion, the catalyst was isolated by centrifugation, washed with THF and introduced in the next cycle. Ten consecutive reactions of phenylacetylene with *p*-nitrobenzyl azide were carried out giving the targeted 1,2,3-triazole in comparable yields (90-98 %) (Figure 6). The content of resting copper derivatives in the final products was determined by using ISP-OES technique. The average value of copper content was found to be of 48 ppm and 15 ppm for the Sonogashira coupling (Table 5, entry 2) and the Huisgen cycloaddition (Table 8, entry 1) reactions, respectively, that is among of the lowest values reported for heterogeneous copper catalysts.<sup>23,121-127</sup>

The morphology of recovered catalysts was also investigated by using SEM microphotography of the solid recovered after the Sonogashira-type coupling performed in toluene in the presence of PPh<sub>3</sub> and strong Cs<sub>2</sub>CO<sub>3</sub> base. As seen in Figure 7, a morphology of **Cu/6b/SM/A** remains intact after the reaction completion and the powder is composed of uniform agglomerates of primary nanoparticles.

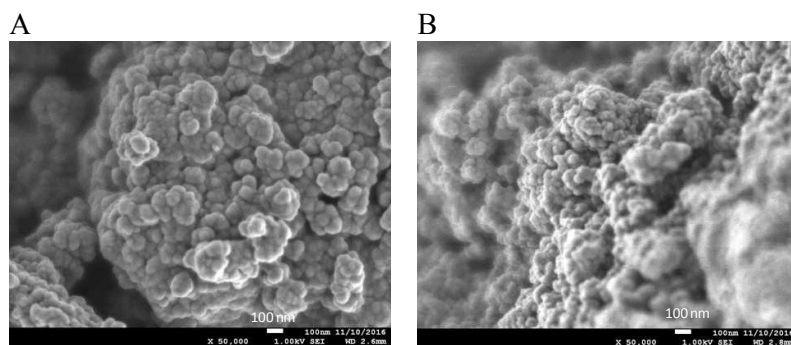


**Figure 7.** SEM microphotographs of solid **Cu/6b/SM/A** (A), and the recycled catalyst after Sonogashira coupling (B). The images were obtained using samples prepared by the dispersion the materials on a conductive carbon tape and carbon coating (8 nm).

## Conclusions

In the present work, different strategies for the covalent immobilization of copper complexes with **pphen** ligands functionalized by phosphonate groups (**Pphen**) were systematically explored. Reported SG methods for the preparation of titania-supported transition metal complexes were compared to the SM of hydrated mesoporous titania that we have synthesized recently. The resulting hybrid materials were characterized as both a bulk solids and at the molecular level by using different physicochemical methods including elemental analysis, infrared spectroscopy, nitrogen sorption isotherms, SEM microphotography.

Immobilization of labile heteroleptic copper(I) complexes with **Pphen** ligands is accompanied by a partial removal of metal ions whatever the experimental procedure was used for the covalent link of these complexes to TiO<sub>2</sub> supports. This drawback can be overcome by using the stepwise method involving the immobilization of **Pphen-Si** ligands and their consecutive complexation with copper(I) ions. Most porous material **Cu/6b/SM/A** in which **Pphen** ligand is linked to the surface by a single phosphonate group located at 3-position of the phenanthroline backbone and coordinated to copper(I) ions was prepared by the post-synthetic modification of hydrated mesoporous TiO<sub>2</sub> ( $S_{\text{BET}} = 650 \text{ m}^2 \text{ g}^{-1}$ ). This material exhibits BET surface area of  $246 \text{ m}^2 \text{ g}^{-1}$ , contains 0.57 mmol of the grafted complex

per gram of the solid and benefits from the high thermal and chemical robustness, the nanosized morphology, the mesoporosity and the spatial separation of catalytic sites.

Excellent catalytic performance of **Cu/6b/SM/A** in the Sonogashira-type coupling and the Huisgen 1,3-dipolar cycloaddition was also demonstrated. Fairly low catalyst loading, a simple recovery and reuse of the solid were achieved in both studied reactions proceeding through principally different reaction pathways. This catalytic versatility of copper catalyst is highly desirable for sustainable chemistry but still rarely reported owing to the challenge in the preparation of robust catalysts applicable for a wide range of experimental conditions. Our ongoing work focuses on the screening of catalytic reactions promoted by **Cu/6b/SM/A**. This work also paves the way towards cost-effective heterogenized transition metal catalysts prepared by grafting of metal complexes decorated by phosphonate anchoring groups onto the surface of mesoporous TiO<sub>2</sub> that we have prepared recently according the non-templating sol-gel process.

## Acknowledgements

Myriam Heydel, Fanny Picquet and Marcel Soustelle are warmly acknowledged for their technical support. The authors are very grateful to Remi Chassagnon for the cooperation in TEM studies and helpful discussions. A.Yu. Mitrofanov thanks the Russian Foundation for Basic Research (grant No. 16-33-60207) for the financial support and the French government for PhD fellowship. Financial support from the CNRS and the Burgundy Region (PARI IME SMT8 and PARI II CDEA programs) is also acknowledged. This work was carried out in the frame of the International Associated French–Russian (LIA) Laboratory of Macrocyclic Systems and Related Materials (LAMREM) of CNRS and RAS.

## References

1. G. Evano, N. Blanchard and M. Toumi, *Chem. Rev.*, 2008, **108**, 3054-3131.
2. *Copper-Mediated Cross-Coupling Reactions*, eds. G. Evano and N. Blanchard, Wiley, Hoboken, 2013, 840pp.
3. P. Subramanian, G. C. Rudolf and K. P. Kaliappan, *Chem.—Asian J.*, 2016, **11**, 168-192.
4. *C-H and C-X Bond Functionalization: Transition Metal Mediation*, ed. X. Ribas, RSC Publishing, Cambridge, 2013, 350 pp.
5. F. Monnier and M. Taillefer, in *Amination and Formation of  $sp^2$  C-N Bonds*, eds. M. Taillefer and D. Ma, Springer, Berlin, Heidelberg, 2013, pp. 173-204.
6. A. P. Jadhav, D. Ray, V. U. B. Rao and R. P. Singh, *Eur. J. Org. Chem.*, 2016, 2369-2382.
7. C. Maaliki, E. Thiery and J. Thibonnet, *Eur. J. Org. Chem.*, 2016, 209-228.
8. I. P. Beletskaya and A. V. Cheprakov, *Organometallics*, 2012, **31**, 7753-7808.
9. Y. Shimizu and M. Kanai, *Tetrahedron Lett.*, 2014, **55**, 3727-3737.
10. V. Castro, H. Rodríguez and F. Albericio, *ACS Combinatorial Science*, 2016, **18**, 1-14.
11. A. S. Hay, *J. Org. Chem.*, 1962, **27**, 3320-3321.

12. G. W. Kabalka, L. Wang and R. M. Pagni, *Synlett*, 2001, 108-110.
13. J. S. Yadav, B. V. S. Reddy, K. B. Reddy, K. U. Gayathri and A. R. Prasad, *Tetrahedron Lett.*, 2003, **44**, 6493-6496.
14. T. F. Knöpfel and E. M. Carreira, *J. Am. Chem. Soc.*, 2003, **125**, 6054-6055.
15. K. Kamata, S. Yamaguchi, M. Kotani, K. Yamaguchi and N. Mizuno, *Angew. Chem., Int. Ed.*, 2008, **13**, 2407-2410.
16. *Copper in drinking-water*. Background document for development of WHO guidelines for drinking-water quality, 2004.
17. V. Balaram, *Trends Anal. Chem.*, 2016, **80**, 83-95.
18. M. B. Gawande, A. Goswami, F.-X. Felpin, T. Asefa, X. Huang, R. Silva, X. Zou, R. Zboril and R. S. Varma, *Chem. Rev.*, 2016, **116**, 3722-3811.
19. M. Keller, M. Ianchuk, S. Ladeira, M. Taillefer, A. M. Caminade, J. P. Majoral and A. Ouali, *Eur. J. Org. Chem.*, 2012, 1056-1062.
20. C.-K. Chen, Y.-W. Chen, C.-H. Lin, H.-P. Lin and C.-F. Lee, *Chem. Commun.*, 2010, **46**, 282-284.
21. A. Coelho, P. Diz, O. Caamaño and E. Sotelo, *Adv. Synth. Catal.*, 2010, **352**, 1179-1192.
22. R. Arundhathi, D. C. Kumar and B. Sreedhar, *Eur. J. Org. Chem.*, 2010, 3621-3630.
23. K. R. Reddy, N. S. Kumar, B. Sreedhar and M. L. Kantam, *J. Mol. Catal. A: Chem.*, 2006, **252**, 136-141.
24. M. L. Kantam, B. P. C. Rao, B. M. Choudary and R. S. Reddy, *Synlett*, 2006, 2195-2198.
25. S. M. Auer, M. Schneider and A. Baiker, *J. Chem. Soc., Chem. Commun.*, 1995, 2057-2058.
26. P. Yu, Y. Zhou, Y. Yang and R. Tang, *RSC Adv.*, 2016, **6**, 65403-65411.
27. B. M. Choudary, C. Sridhar, M. L. Kantam and B. Sreedhar, *Tetrahedron Lett.*, 2004, **45**, 7319-7321.
28. B. M. Choudary, C. Sridhar, M. L. Kantam, G. T. Venkanna and B. Sreedhar, *J. Am. Chem. Soc.*, 2005, **127**, 9948-9949.
29. F. Boccuzzi, G. Martra, C. P. Papalia and N. Ravasio, *J. Catal.*, 1999, **184**, 327-334.
30. M. P. Pachamuthu, S. Karthikeyan, R. Maheswari, A. F. Lee and A. Ramanathan, *Appl. Surf. Sci.*, 2017, **393**, 67-73.
31. F. Zaccheria, N. Ravasio, A. Fusi, M. Rodondi and R. Psaro, *Adv. Synth. Catal.*, 2005, **347**, 1267-1272.
32. F. Zaccheria, N. Ravasio, R. Psaro and A. Fusi, *Chem.—Eur. J.*, 2006, **12**, 6426-6431.
33. I. S. Park, M. S. Kwon, Y. Kim, J. S. Lee and J. Park, *Org. Lett.*, 2008, **10**, 497-500.
34. S. Bhadra, B. Sreedhar and B. C. Ranu, *Adv. Synth. Catal.*, 2009, **351**, 2369-2378.
35. B. H. Lipshutz and B. R. Taft, *Angew. Chem., Int. Ed.*, 2006, **45**, 8235-8238.
36. T. Oishi, K. Yamaguchi and N. Mizuno, *ACS Catalysis*, 2011, **1**, 1351-1354.
37. P. Tepmatee and P. Siriphannon, *Bull. Pol. Acad. Sci., Tech. Sci.*, 2016, **64**, 553-560.
38. M. Bhardwaj, M. Kour and S. Paul, *RSC Adv.*, 2016, **6**, 99604-99614.
39. W. Cao, H. Zhang and Y. Yuan, *Catal. Lett.*, 2003, **91**, 243-246.
40. W. Chen, Y. Zhang, L. Zhu, J. Lan, R. Xie and J. You, *J. Am. Chem. Soc.*, 2007, **129**, 13879-13886.
41. A. Megia-Fernandez, M. Ortega-Muñoz, J. Lopez-Jaramillo, F. Hernandez-Mateo and F. Santoyo-Gonzalez, *Adv. Synth. Catal.*, 2010, **352**, 3306-3320.
42. D. R. Godhani, H. D. Nakum, D. K. Parmar, J. P. Mehta and N. C. Desai, *Inorg. Chem. Commun.*, 2016, **72**, 105-116.
43. J.-C. Wang, Y.-H. Hu, G.-J. Chen and Y.-B. Dong, *Chem. Commun.*, 2016, **52**, 13116-13119.

44. S. Behrouz and M. N. S. Rad, *ChemInform*, 2016, **47**, 10.1002/chin.201620132.
45. T. Miao and L. Wang, *Synthesis*, 2008, 363-368.
46. P. Li and L. Wang, *Tetrahedron*, 2007, **63**, 5455-5459.
47. L. Wang, P. Li and L. Zhang, *Lett. Org. Chem.*, 2006, **3**, 282-285.
48. M. Islam, S. Mondal, P. Mondal, A. S. Roy, K. Tuhina, M. Mobarok, S. Paul, N. Salam and D. Hossain, *Catal. Lett.*, 2011, **141**, 1171-1181.
49. C. e. Queffelec, M. Petit, P. Janvier, D. A. Knight and B. Bujoli, *Chem. Rev.*, 2012, **112**, 3777-3807.
50. G. Guerrero, J. G. Alauzun, M. Granier, D. Laurencin and P. H. Mutin, *Dalton Trans.*, 2013, **42**, 12569-12585.
51. Y.-P. Zhu, T.-Z. Ren and Z.-Y. Yuan, *Catal. Sci. Technol.*, 2015, **5**, 4258-4279.
52. P. Bhanja and A. Bhaumik, *ChemCatChem*, 2016, **8**, 1607-1616.
53. C. Maillet, P. Janvier, M. Pipelier, T. Praveen, Y. Andres and B. Bujoli, *Chem. Mater.*, 2001, **13**, 2879-2884.
54. A. Vioux, J. le Bideau, P. H. Mutin and D. Leclercq, *Top. Curr. Chem.*, 2004, **232**, 145-174.
55. Y.-P. Zhu, T.-Y. Ma, Y.-L. Liu, T.-Z. Ren and Z.-Y. Yuan, *Inorg. Chem. Front.*, 2014, **1**, 360-383.
56. G. Guerrero, P. H. Mutin, E. Framery and A. Vioux, *New J. Chem.*, 2008, **32**, 1519-1525.
57. C. Maillet, P. Janvier, M.-J. Bertrand, T. Praveen and B. Bujoli, *Eur. J. Org. Chem.*, 2002, 1685-1689.
58. T. L. Schull, L. Henley, J. R. Deschamps, R. J. Butcher, D. P. Maher, C. A. Klug, K. Swider-Lyons, W. J. Dressick, B. Bujoli, A. E. Greenwood, L. K. B. Congiardo and D. A. Knight, *Organometallics*, 2007, **26**, 2272-2276.
59. R. Gujadhur, D. Venkataraman and J. T. Kintigh, *Tetrahedron Lett.*, 2001, **42**, 4791-4793.
60. D. Tzalis and Y. Tor, *Tetrahedron Lett.*, 1995, **36**, 6017-6020.
61. C. Dietrich-Buchecker, B. Colasson, D. Jouvenot and J.-P. Sauvage, *Chem.—Eur. J.*, 2005, **11**, 4374-4386.
62. T. Ishiyama, M. Murata and N. Miyaura, *J. Org. Chem.*, 1995, **60**, 7508-7510.
63. N. N. Makukhin, PhD, Lomonosov Moscow State University, 2013.
64. A. Mitrofanov, A. Bessmertnykh Lemeune, C. Stern, R. Guillard, N. Gulyukina and I. Beletskaya, *Synthesis*, 2012, **44**, 3805-3810.
65. A. Mitrofanov, M. Manowong, Y. Rousselin, S. Brandes, R. Guillard, A. Bessmertnykh-Lemeune, P. Chen, K. M. Kadish, N. Goulioukina and I. Beletskaya, *Eur. J. Inorg. Chem.*, 2014, 3370-3386.
66. H. E. Gottlieb, V. Kotlyar and A. Nudelman, *J. Org. Chem.*, 1997, **62**, 7512-7515.
67. G. R. Fulmer, A. J. M. Miller, N. H. Sherden, H. E. Gottlieb, A. Nudelman, B. M. Stoltz, J. E. Bercaw and K. I. Goldberg, *Organometallics*, 2010, **29**, 2176-2179.
68. S. Brunauer, P. H. Emmett and E. Teller, *J. Am. Chem. Soc.*, 1938, **60**, 309-319.
69. E. P. Barrett, L. G. Joyner and P. P. Halenda, *J. Am. Chem. Soc.*, 1951, **73**, 373-380.
70. S. B. Park and H. Alper, *Chem. Commun.*, 2004, 1306-1307.
71. S. Wang, M. Wang, L. Wang, B. Wang, P. Li and J. Yang, *Tetrahedron*, 2011, **67**, 4800-4806.
72. H. Peng, Y.-Q. Chen, S.-L. Mao, Y.-X. Pi, Y. Chen, Z.-Y. Lian, T. Meng, S.-H. Liu and G.-A. Yu, *Org. Biomol. Chem.*, 2014, **12**, 6944-6952.
73. C. J. Wenthur, R. Morrison, A. S. Felts, K. A. Smith, J. L. Engers, F. W. Byers, J. S. Daniels, K. A. Emmitte, P. J. Conn and C. W. Lindsley, *J. Med. Chem.*, 2013, **56**, 5208-5212.

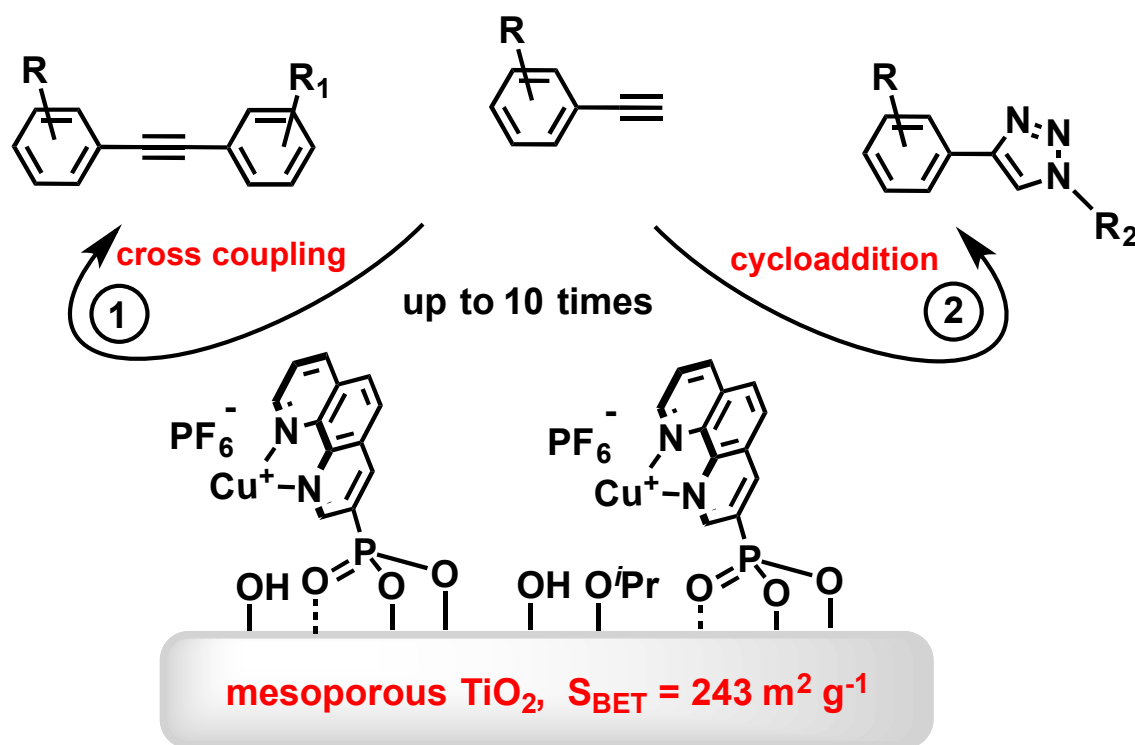


74. S. Kankala, R. Vadde and C. S. Vasam, *Org. Biomol. Chem.*, 2011, **9**, 7869-7876.
75. H. Kim and P. H. Lee, *Adv. Synth. Catal.*, 2009, **351**, 2827-2832.
76. S. S. E. Ghodsinia, B. Akhlaghinia and R. Jahanshahi, *RSC Adv.*, 2016, **6**, 63613-63623.
77. R. Jahanshahi and B. Akhlaghinia, *RSC Adv.*, 2016, **6**, 29210-29219.
78. S. Ladouceur, A. M. Soliman and E. Zysman-Colman, *Synthesis*, 2011, 3604-3611.
79. H. Xu and Z. Sun, *Adv. Synth. Catal.*, 2016, **358**, 1736-1740.
80. O. I. Artyushin, D. V. Vorob'eva, T. P. Vasil'eva, S. N. Osipov, G.-V. Roschenthaler and I. L. Odinets, *Heteroat. Chem.*, 2008, **19**, 293-300.
81. A. Y. Mitrofanov, A. G. Bessmertnykh-Lemeune and I. P. Beletskaya, *Inorg. Chim. Acta*, 2015, **431**, 297-301.
82. P. M. DiGiacomo and M. B. Dines, *US* 4299943, 1981.
83. G. Guerrero, P. H. Mutin and A. Vioux, *Chem. Mater.*, 2001, **13**, 4367-4373.
84. M. Mehring, V. Lafond, P. H. Mutin and A. Vioux, *J. Sol-Gel Sci. Technol.*, 2003, **26**, 99-102.
85. N. R. E. Radwan, M. Mokhtar and G. A. El-Shobaky, *J. Therm. Anal. Calorim.*, 2003, **71**, 977-986.
86. G. Li, L. Li, J. Boerio-Goates and B. F. Woodfield, *J. Am. Chem. Soc.*, 2005, **127**, 8659-8666.
87. N. Nakayama and T. Hayashi, *Colloids Surf., A*, 2008, **317**, 543-550.
88. T. P. Gerasimova and S. A. Katsyuba, *Dalton Trans.*, 2013, **42**, 1787-1797.
89. B. Ackerman, T. A. Jordan, C. R. Eddy and D. Swern, *J. Am. Chem. Soc.*, 1956, **78**, 4444-4447.
90. P. Persson, E. Laiti and L.-O. Öhman, *J. Colloid Interface Sci.*, 1997, **190**, 341-349.
91. J. Randon, P. Blanc and R. Paterson, *J. Membr. Sci.*, 1995, **98**, 119-129.
92. A. Raman, R. Quiñones, L. Barriger, R. Eastman, A. Parsi and E. S. Gawalt, *Langmuir*, 2010, **26**, 1747-1754.
93. R. J. H. Clark, C. D. Flint and A. J. Hempleman, *Spectrochim. Acta Mol. Biomol. Spectrosc.*, 1987, **43**, 805-816.
94. D. Geldof, M. Tassi, R. Carleer, P. Adriaensens, A. Roevens, V. Meynen and F. Blockhuys, *Surf. Sci.*, 2017, **655**, 31-38.
95. G. Guerrero, P. H. Mutin and A. Vioux, *Chem. Mater.*, 2000, **12**, 1268-1272.
96. P. H. Mutin, V. Lafond, A. F. Popa, M. Granier, L. Markey and A. Dereux, *Chem. Mater.*, 2004, **16**, 5670-5675.
97. G. Murphy, C. Murphy, B. Murphy and B. Hathaway, *J. Chem. Soc., Dalton Trans.*, 1997, 2653-2660.
98. Y. Yamada, H. Sakurai, Y. Miyashita, K. Fujisawa and K.-i. Okamoto, *Polyhedron*, 2002, **21**, 2143-2147.
99. R. Chinchilla and C. Najera, *Chem. Soc. Rev.*, 2011, **40**, 5084-5121.
100. M. Bakherad, *Appl. Organomet. Chem.*, 2013, **27**, 125-140.
101. A. R. Hajipour and F. Mohammadsaleh, *Tetrahedron Lett.*, 2014, **55**, 3459-3462.
102. J. Moegling, A. D. Benischke, J. M. Hammann, N. A. Veprek, F. Zoller, B. Rendenbach, A. Hoffmann, H. Sievers, M. Schuster, P. Knochel and S. Herres-Pawlis, *Eur. J. Org. Chem.*, 2015, 7475-7483.
103. N. P. Probst, B. Deprez and N. Willand, *Tetrahedron Lett.*, 2016, **57**, 1066-1070.
104. B. W. T. Gruijters, M. A. C. Broeren, F. L. van Delft, R. P. Sijbesma, P. H. H. Hermkens and F. P. J. T. Rutjes, *Org. Lett.*, 2006, **8**, 3163-3166.
105. A. Biffis, E. Scattolin, N. Ravasio and F. Zaccheria, *Tetrahedron Lett.*, 2007, **48**, 8761-8764.
106. Z. Wang, L. Wang and P. Li, *Synthesis*, 2008, 1367-1372.

107. A. R. Hajipour, S. M. Hosseini and F. Mohammadsaleh, *New J. Chem.*, 2016, **40**, 6939-6945.
108. L.-j. Bai, W.-x. Wang, M.-h. Wang, J.-m. Sun and H. Chen, *Chin. J. Polym. Sci.*, 2015, **33**, 1260-1270.
109. *Click Chemistry for Biotechnology and Materials Science*, ed. J. Lahann, Wiley, Chichester, 2009, 411 pp.
110. V. Castro, H. Rodriguez and F. Albericio, *ACS Comb. Sci.*, 2016, **18**, 1-14.
111. J.-P. Meyer, P. Adumeau, J. S. Lewis and B. M. Zeglis, *Bioconjugate Chem.*, 2016, **27**, 2791-2807.
112. X.-P. He, Y.-L. Zeng, Y. Zang, J. Li, R. A. Field and G.-R. Chen, *Carbohydr. Res.*, 2016, **429**, 1-22.
113. K. Kacprzak, I. Skiera, M. Piasecka and Z. Paryzek, *Chem. Rev.*, 2016, **116**, 5689-5743.
114. V. K. Tiwari, B. B. Mishra, K. B. Mishra, N. Mishra, A. S. Singh and X. Chen, *Chem. Rev.*, 2016, **116**, 3086-3240.
115. C. Wang, D. Ikhlef, S. Kahlal, J.-Y. Saillard and D. Astruc, *Coord. Chem. Rev.*, 2016, **316**, 1-20.
116. M. S. Singh, S. Chowdhury and S. Koley, *Tetrahedron*, 2016, **72**, 5257-5283.
117. C. Girard, E. Önen, M. Aufort, S. Beauvière, E. Samson and J. Herscovici, *Org. Lett.*, 2006, **8**, 1689-1692.
118. I. Jalia, H. Elamari, F. Meganem, J. Herscovici and C. Girard, *Tetrahedron Lett.*, 2008, **49**, 6756-6758.
119. P. Li, L. Wang and Y. Zhang, *Tetrahedron*, 2008, **64**, 10825-10830.
120. H. Sharghi, R. Khalifeh and M. M. Doroodmand, *Adv. Synth. Catal.*, 2009, **351**, 207-218.
121. M. Ercoli, A. Fusi, R. Psaro, N. Ravasio and F. Zaccheria, *J. Mol. Catal. A: Chem.*, 2003, **204-205**, 729-735.
122. P. R. Likhar, S. Roy, M. Roy, M. L. Kantam and R. L. De, *J. Mol. Catal. A: Chem.*, 2007, **271**, 57-62.
123. S. Benyahya, F. Monnier, M. Taillefer, M. W. C. Man, C. Bied and F. Ouazzani, *Adv. Synth. Catal.*, 2008, **350**, 2205-2208.
124. S. Benyahya, F. Monnier, M. Wong Chi Man, C. Bied, F. Ouazzani and M. Taillefer, *Green Chemistry*, 2009, **11**, 1121-1123.
125. W. Mo, H. Liu, H. Xiong, M. Li and G. Li, *Appl. Catal., A*, 2007, **333**, 172-176.
126. P. Ling, D. Li and X. Wang, *J. Mol. Catal. A: Chem.*, 2012, **357**, 112-116.
127. P. Zhang, J. Yuan, H. Li, X. Liu, X. Xu, M. Antonietti and Y. Wang, *RSC Adv.*, 2013, **3**, 1890-1895.

## Immobilization of copper complexes with (1,10-phenanthrolyl)phosphonates on titania supports for sustainable catalysis

A. Mitrofanov, S. Brandès, F. Herbst, S. Rigolet, A. Bessmertnykh-Lemeune,\* I. Beletskaya\*



Different immobilization strategies were explored to prepare mesoporous titania-supported copper complexes with 1,10-phenanthroline functionalized by the phosphonate anchoring group. A cost-effective, robust, recovered and reusable catalyst for Sonogashira-type and Huisgen cycloaddition reactions was developed.